Current Forestry Reports
https://doi.org/10.1007/s40725-023-00207-z

REMOTE SENSING (J SUAREZ, SECTION EDITOR)

Thermal Infrared Remote Sensing of Stress Responses in Forest Environments: a Review of Developments, Challenges, and Opportunities

Magdalena Smigaj[1] · Avinash Agarwal[2] · Harm Bartholomeus[1] · Mathieu Decuyper[3] · Ahmed Elsherif[4] · Arjen de Jonge[1,3] · Lammert Kooistra[1]

Accepted: 10 November 2023

Abstract

Purpose of Review The successful application of thermal infrared (TIR) remote sensing in the agricultural domain, largely driven by the arrival of new platforms and sensors that substantially increased thermal data resolution and availability, has sparked interest in thermography as a tool for monitoring forest health. In this review, we take a step back to reflect on what physiological responses are reflected in leaf and canopy temperature and summarise research activities on TIR remote sensing of stress responses in forest environments, highlighting current methodological challenges, open questions, and promising opportunities.

Recent Findings This systematic literature review showed that whilst the focus still remains on satellite imagery, Uncrewed Aerial Vehicles (UAVs) are playing an increasingly important role in testing the capabilities and sensitivity to stress onset at the individual tree level. To date, drought stress has been the focal point of research, largely due to its direct link to stomatal functioning at leaf level. Though, research into thermal responses to other stressors, e.g. pathogens, is also gaining momentum.

Summary Disentangling stress-induced canopy temperature variations from environmental factors and structural influences remains the main challenge for broader application of TIR remote sensing. Further development and testing of approaches for thermal data analysis, including their applicability for different tree species and sensitivity under different climatic conditions, are required to establish how TIR remote sensing can best complement existing forest health monitoring approaches.

Keywords Thermal infrared remote sensing · Thermography · Canopy temperature · Forest health · Stress response · Vegetation

Introduction

Abnormal temperature deviations have long been known to be reflective of ailments in living beings. In healthcare settings, temperature measurements are taken as part of the regular routine checks of vital signs to help understand the health status and detect infection onset early. In plants, leaf temperature deviations are similarly reflective of physiological changes and can be used as early indicators of disruptions to plant functioning. The links between leaf temperature and its functioning are well known and have long been investigated in both laboratory and outdoor settings using thermal sensors: various studies on crops have linked leaf temperature to stomatal conductance and have demonstrated its feasibility for identifying drought stress [1–4] and pre-visual disease symptoms [5–8]. Yet, the

✉ Magdalena Smigaj
magdalena.smigaj@wur.nl

1 Laboratory of Geo-Information Science and Remote Sensing, Wageningen University & Research, Droevendaalsesteeg 3, 6708 PB Wageningen, the Netherlands

2 School of Natural and Environmental Sciences, Newcastle University, Newcastle Upon Tyne NE1 7RU, UK

3 Forest Ecology & Forest Management Group, Wageningen University & Research, Droevendaalsesteeg 3, 6708 PB Wageningen, the Netherlands

4 Faculty of Engineering, Tanta University, Tanta, Egypt

Published online: 08 December 2023

applicability of thermography for stress onset detection and health monitoring purposes in forest environments remains scarcely explored.

Thermal sensors measure the amount of radiation emitted from observed surfaces, which subsequently can be converted to temperature readings. They operate in the thermal infrared (TIR) region of the electromagnetic spectrum, which occupies wavelengths from 3 to 14 µm; however, due to atmospheric absorption, only two regions can effectively be utilised: 3–5 µm (MWIR) and 8–14 µm (LWIR) with the latter being typically used for remote sensing applications since daytime thermal MWIR imagery can be contaminated by reflected sunlight and require additional corrections. The origins of thermal infrared (TIR) remote sensing can be traced back to the 1960s when the TIROS-2 satellite, equipped with an infrared thermometer, was launched into orbit [9]. Since then, TIR remote sensing has proliferated with a range of existing satellite missions featuring sensors with thermal bands (e.g. Landsat, MODIS, ECOSTRESS) and a number of private ventures launched with the aim of tackling the limitations of existing satellite TIR imaging capabilities in the near future (e.g. Orora technologies, Hydrosat, Contellr).

The applications of TIR remote sensing are very broad, including climatology, hydrology, agronomy, and ecology. In forest settings, most focus has so far been put on detection, study, and management of biomass burning; a range of active fire detection methods have been developed over the years [10–12], and operational active fire products are now available in near-real time to aid fire management (e.g. [13, 14]). The use of thermal imagery for fire burn mapping, estimation of live fuel moisture content, and fire risk assessment has also been explored [12, 15–17]. Though, in the latter case, remotely sensed surface temperature has generally been used as an environmental variable indicating the onset and occurrence of dry conditions rather than as an indicator of health status.

The arrival of new platforms and sensors, which increased spatial resolution (from hundreds of metres to several decimetres) and availability of thermal data, together with their successful application in the agricultural domain (e.g. [18–22]) has sparked interest in TIR remote sensing as a tool for detecting and assessing stress responses in forests. The number of studies on this topic has markedly increased since around 2005 (Fig. 1), with many of the earlier publications being review articles that were only highlighting this potential. Although the research focus still remains on satellite imagery, Uncrewed Aerial Vehicles (UAVs) are playing an increasingly important role in testing the capabilities and sensitivity to stress onset at individual tree level, providing high spatial resolution data at a fraction of the cost of airborne campaigns (for local case studies). Additionally, Fig. 1 highlights that drought stress, largely due to its direct link to stomatal functioning at leaf level, has so far been the focal point of research in forests. Nonetheless, thermal responses to other stressors are also starting to be researched; we identified 15 studies that investigated other specific stressors, out of which 14 focused on infections and infestations and 1 on frost damage. This shows the desire to better understand what is possible and feasible with TIR remote sensing and how it can complement existing forest health monitoring approaches.

Here, in response to this interest, we take a step back to reflect on what physiological responses are reflected in leaf and canopy temperature and discuss how TIR remote sensing is currently utilised in forest environments for identification and monitoring of stress. Subsequently, we highlight current methodological challenges, open questions, and promising opportunities for future explorations into the thermal domain. As the use of thermography for applications surrounding forest fires falls outside the scope of this review, readers specifically interested in this topic are instead advised to refer to Szpakowski and Jensen [17], Leblon et al. [12], and Wooster et al. [11], who have already covered this aspect in depth.

Physiological Responses to Stress Onset

Physical and Physiological Aspects of Thermoregulation

Plants exchange heat with the environment continuously, and these thermoregulatory changes can be endothermic (absorbing energy) or exothermic (releasing energy) depending on the state of thermal equilibrium of the plant [23]. Incoming solar radiation is considered the primary source of thermal energy for plants; in the TIR region, it delivers heat to the plant body, whereas in specific visible wavebands, it is absorbed by leaves for photosynthesis [24]. Subsequent breakdown of photosynthates during cellular respiration results in the generation of intrinsic heat within plant tissues [25]. Heat is also generated within leaves when excess light energy is transduced to thermal energy by specific carotenoids for photoprotection via non-photochemical quenching [26]. In addition, longwave radiative heat exchange to and from neighbouring surfaces also accounts for the transfer of thermal energy between a plant and its surroundings [27].

Although persistent, the influence of these processes on sensible plant temperature is masked by transpirational and convective heat transfer [27, 28]. Overall plant temperature is affected remarkably by transpiration via stomatal opening in response to environmental stimuli and stressors (Fig. 2a) [23]. Stomatal opening for the uptake and release of CO_2 and O_2 to facilitate photosynthesis and respiration also leads to evaporation of water from the leaf [29, 30]. When stomata

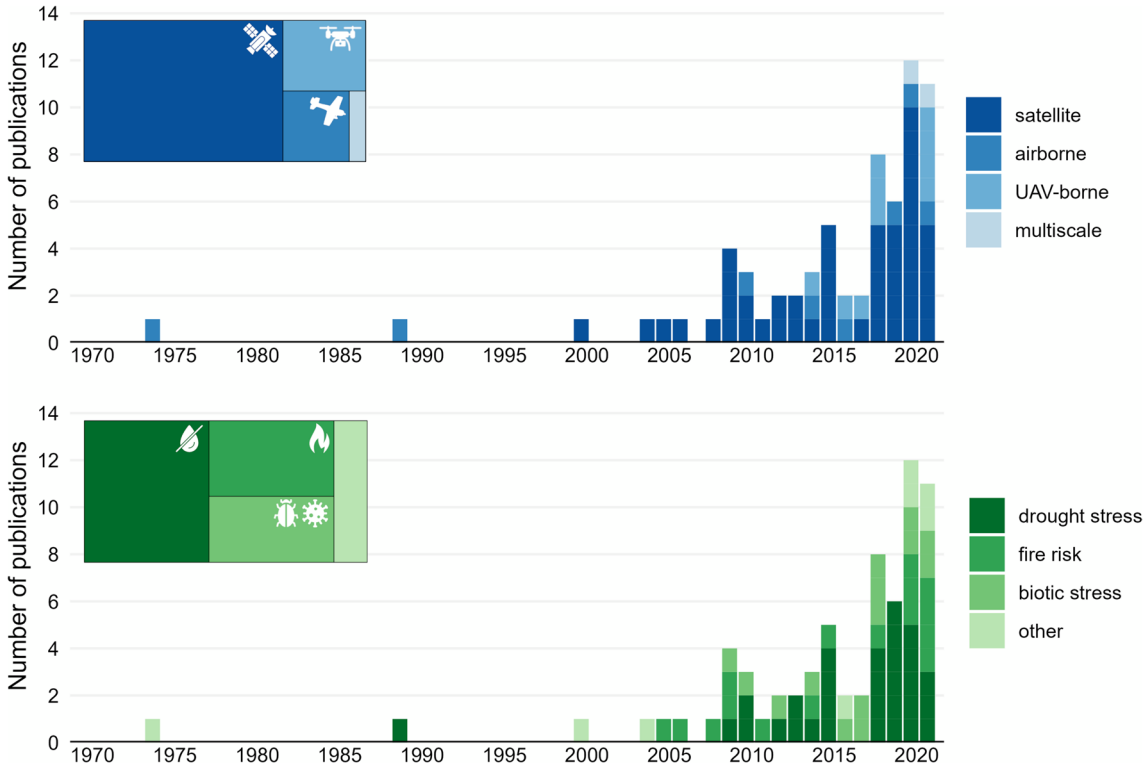

Fig. 1 Number of TIR remote sensing publications (until the end of 2022) focusing on detection and assessment of stress responses in forests, categorised by the imaging platform (*top*) and the topic (*bottom*). The counts are based on systematic literature search results from Web of Science and Scopus—a summary of the literature search and exclusion criteria is provided in the Supplementary Material. Note: 'multiscale' refers to studies that used data from multiple platforms, whilst 'other' refers to review publications and otherwise unattributed studies. It should also be noted that in the case of fire risk assessment studies, we excluded publications where surface temperature was used as an environmental variable rather than as an indicator of health status

open, water molecules near the stomatal aperture absorb energy from the surrounding tissue, generating the latent heat of transpiration and enabling the water molecules to overcome leaf boundary layer resistance and escape, resulting in rapid cooling of the leaf [27, 30]. Herein, the leaf boundary layer refers to the thin layer of calm air adjacent to the leaf surface that influences how quickly gases and energy are exchanged between the leaf and the surrounding air, with thicker layers leading to reduced transfer of heat, CO_2, and water vapour [31]. Since the thickness of the leaf boundary layer tends to increase with leaf size, heat is transferred faster in smaller leaves, which leads to their equilibrium temperatures being closer to the ambient air compared to larger leaves [32]. This effect was illustrated via substantial differences in heat transfer between broadleaf and needleleaf trees [33] with needleleaf species exhibiting considerably smaller leaf-to-air temperature differences (0.3–2.8 °C) than broadleaf species (4.5–4.8 °C) [33]. Other factors such as sunlight, wind speed, humidity, air temperature, and respiration influence transpirational cooling rates across a tree crown dynamically (Fig. 2b); for instance, fully-exposed sun-lit leaves in the upper canopy are typically exposed to higher temperatures and have higher transpirational cooling rates compared to partially shaded leaves lower in the crown [34, 35]. These differences, however, also depend on canopy structure, which affects aerodynamics, and consequently the transfer of heat via convection [36].

Convective heat exchange occurs passively when air molecules in contact with the plant surface act as a medium for transferring heat to and from the atmosphere to maintain thermal equilibrium (Fig. 2e). During this process, the role of leaves predominates compared to the trunk and woody branches due to the insulating nature of wood and bark, as well as the evolutionary design of the trunk in the form of a cylinder, which minimises surface area to volume ratio for heat exchange [37]. Canopy architectural traits such as leaf density, branching pattern, and vertical distribution of leaves play a crucial role in temperature regulation via convective heat exchange (Fig. 2e) [33]. As indicated by studies on various tree species, compact canopies, i.e. having high leaf density, dissipate heat slowly and appear warm, whereas trees with relatively open canopies tend to have equal or lower temperatures compared to ambient [33, 38]. This trend in convective heat transfer may be extrapolated to total canopy

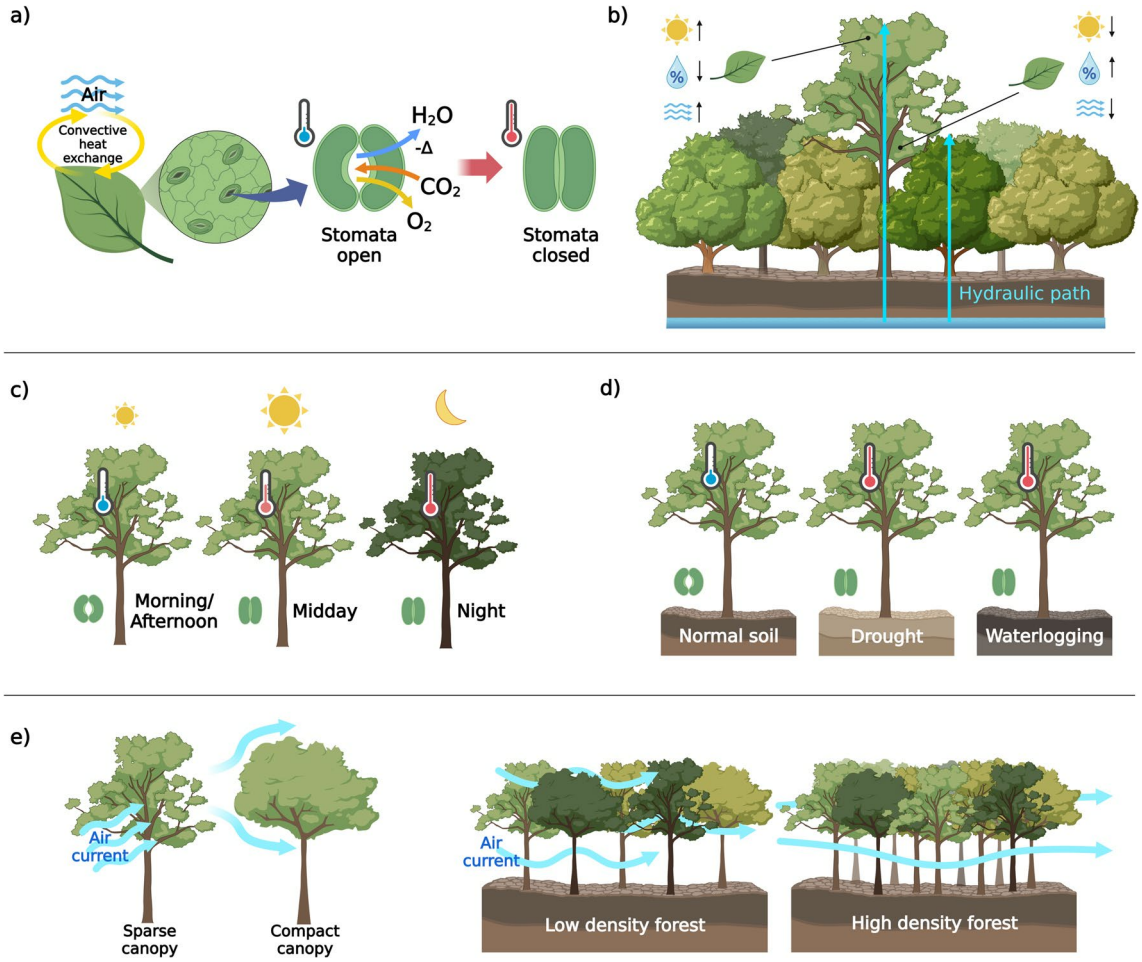

Fig. 2 Schematic diagram summarising plant thermoregulation concepts. **a** Leaves maximise surface area for heat exchange through convection and actively regulate overall plant temperature by controlling transpiration in response to external stimuli. **b** Rate of transpiration therefore varies within and between canopies depending on the level of exposure to environmental factors (solar radiation, humidity, air temperature), i.e. leaves in upper vs. lower canopy and emergent trees vs. non-emergent neighbours. **c** In normal conditions, stomata open in response to sunlight. Though, when irradiation reaches high levels, stomata tend to close to avoid photosynthetic photooxidative stress, which leads to reduced transpirational cooling. **d** Stress onset typically triggers stomatal closure. During drought, it occurs due to reduced hydraulic conductance, whereas during flooding, it is a systemic response to root anoxia. **e** Canopy architectural traits and forest characteristics also play a role in determining canopy temperature since they affect temperature regulation via convective heat exchange by directly influencing aerodynamics

cover. In closed canopies, a smaller proportion of the tree crown is exposed to direct sunlight and air movement due to partial shading by neighbouring trees. Whereas in more open canopies, wind turbulence is higher, which may lead to higher leaf transpiration creating a greater potential for heat dissipation. To what degree these factors affect canopy temperature is strongly dependent on water availability and the influence of immediate surroundings on the microclimate (e.g. forest edge vs continuous forest canopy).

Level of hydration is a predominant factor that impacts plant temperature by directly influencing stomatal movement for regulating transpiration as a 'water retention reflex'. Reduction in turgor pressure within the plant due to low moisture availability results in the shrinking of guard cells and consequently the stomatal aperture, ultimately resulting in reduced transpirational cooling [39]. Low relative humidity, high vapour pressure deficit, and wind promote evaporative water loss and, hence, tend to trigger stomatal closure [39–42]. In contrast, very high relative humidity may reduce transpirational cooling by directly deterring evaporation. Abscisic acid (ABA), a phytohormone involved in various stress responses, plays a crucial role in stomatal closure in response to environmental stimuli by inducing osmotic water efflux from the guard cells to regulate water loss [43, 44]. Regulation of temperature via transpiration in response to these environmental changes may vary markedly depending on the sensitivity of stomatal conductance in different species and must be considered when using

thermography. For instance, isohydric plant species ration water content by adopting a 'water conservation' behaviour, whereas anisohydric plants display a 'risk-taking' behaviour by allowing leaf water potential to drop very low. Hence, stomatal responses in isohydric plant species are more rapid compared to anisohydric plants [45]. At canopy level, differences in responses between individual trees occur due to variations in hydraulic path length, i.e. the distance over which water is transported from roots to individual leaves (Fig. 2b). Sensitivity to water shortages increases with the hydraulic path length; hence, larger trees have a higher risk of embolism formation and mortality [46–48]. In addition, emergent trees have a larger proportion of their crown exposed, experiencing higher wind speeds and irradiance levels compared to their non-emergent neighbours (Fig. 2b). Consequently, they operate more closely to their critical leaf temperature, further increasing their sensitivity to drought and/or heatwaves [46–48].

Thermoregulation in Response to Cyclic Environmental Changes and Stress

Canopy temperature varies considerably following diurnal and seasonal patterns in response to changing environmental conditions (Fig. 2c, d) [49–51]. In forests, it is tightly coupled to air temperature and will follow similar diurnal and seasonal trends [52]. This is in contrast to short vegetation, such as agricultural crops, which experience greater fluctuations, often considerably deviating from ambient temperature. Apart from these anticipated environmental variations, plant thermoregulation also occurs in response to various abiotic and biotic stresses [23, 53, 54]. In general, all such responses are regulated by a network of signalling events mediated by various genes and plant growth regulators [43, 44]. Under normal conditions, stomata open in response to sunlight for photosynthetic gas exchange and transpiration, with the process being reversed at night [55, 56]. Thus, in thermal imagery, a healthy, photosynthesising canopy generally appears cooler than a stressed canopy due to undisturbed transpirational cooling [39, 57]. However, stomata close under high light conditions, occurring naturally when the sun is at its peak, to avoid photosynthetic photooxidative stress. This results in a 'midday depression' in photosynthesis and stomatal gas exchange [52, 58], potentially leading to reduced transpirational cooling in addition to excess radiative heat gain resulting in a significant change in canopy temperature.

Like light, ambient temperature affects canopy thermal signature by influencing stomatal opening. Warm weather encourages stomatal opening to promote transpiration for alleviating heat stress [59]. However, excessive evaporative loss from the soil due to very high air temperatures may indirectly lead to stomatal closure via long-distance ABA signalling initiated by osmotic stress in the roots [60]. This phenomenon is frequently observed in drought-stressed canopies and is noticeable as a spike in temperature [23, 38, 39]. Flooding of the roots also triggers stomatal closure by stress signalling due to root anoxia [53, 61]. Although detrimental during summer, this reduction in stomatal conductance to deter transpiration was found to help herbaceous plants conserve heat and moisture during winter [60, 62]. Though, how different stress intensities and coping mechanisms affect thermal patterns of evergreen species in wintertime still remains unexplored.

In general, retention of moisture and heat by stomatal closure occurs at the cost of photosynthetic activity, and vice versa. Since leaf senescence due to seasonal changes or stress essentially involves sustained ABA signalling for stomatal closure to pause photosynthesis [43], it may be tracked reliably as the change in leaf temperature, which manifests before other symptoms. Biotic stress due to disease and herbivory was also found to increase plant temperature in crops by triggering stomatal closure [23, 63]; salicylic acid, an endogenous plant growth regulator and defensive compound that promotes stomatal closure, has been frequently reported to be upregulated in response to various biotic stressors [64]. Thermal fluctuations under biotic stress may be detected as localised (leaf level) or canopy-wide responses depending upon the nature and level of stress. Root damage caused by viruses, fungal or bacterial pathogens, and root nematodes have the potential to elicit systemic symptoms due to water scarcity and widespread stomatal closure and may cause canopy-level thermal responses. In contrast, temperature change caused by foliar diseases and herbivory or mechanical injury may be more localised depending on the extent of damage. Although well documented in crops, such responses have not been studied extensively in forest species. However, positive reports on various fruit trees indicate the feasibility of thermal imaging for biotic stress detection in forest species [63].

Developments and Trends in TIR Remote Sensing of Stress Responses in Forest Ecosystems

TIR Remote Sensing Concepts and Technologies

TIR sensors principally measure thermal radiance emitted by the land surface, where the incoming solar radiation interacts with the ground. The resultant imagery typically has coarser spatial resolution than optical imagery due to the low amount of energy reaching the sensor, relative to the amount of radiation reflected at shorter wavelengths. For instance, the spatial resolution of MODIS optical data is 250/500 m and that of TIR data is 1000 m. Similarly, Landsat 9 optical

imagery has a spatial resolution of 30 m, whereas for TIR imagery, it is 100 m (Table 1). Over the years, advances in satellite technology and sensor design have enabled significant improvements in the level of detail captured, with some missions now collecting data at 60 m spatial resolution (Table 1). The upcoming Sentinel LSTM mission, planned for launch in 2028, will further improve it to 50 m with a 1–3-day revisit time.

Thermal radiance measured by TIR sensors can subsequently be converted to Land Surface Temperature (LST) by accounting for atmospheric effects on the signal and emissivity properties of the observed surface. Emissivity defines the proportion of energy that a given surface emits relative to a blackbody, a hypothetical perfect radiator that absorbs all incident energy, and then emits it back as heat. Emissivity of real-life materials varies as a function of wavelength and strongly depends on surface type and its properties. Even for leaves, distinctive differences in emissivity spectra can be found between species [78, 79] and across development stages [80]. Richardson et al. [80] found the emissivity value in a number of deciduous tree species to decrease from about 0.99 to 0.95 (across 8–14 μm) as the foliage matured following cuticle development and thickening. Despite these differences, generic emissivity values (of 0.95–0.99 for leaves and 0.98–99 for canopies) obtained from generalised tables are typically used to retrieve plant temperature from broadband thermal imagery, largely due to the shortage of relevant TIR spectral libraries that is being addressed by the ECOSTRESS mission through the collection of vegetation and non-photosynthetic vegetation spectra [81].

Where multiple thermal bands are available, both LST and emissivity can be retrieved through the use of Temperature Emissivity Separation (TES) methods; their performance, however, depends on the number of available thermal bands and accurate elimination of atmospheric effects on the signal [82–85]. Signal-to-noise ratio is a crucial consideration during the design of thermal sensors since the amount of energy emitted in the TIR region is much lower than the amount of energy reflected at shorter wavelengths, significantly restricting achievable spatial resolution. Additionally, with an increasing distance between the sensor and the surface, progressive attenuation of the signal can occur, leading to unique emissivity features becoming weaker or disappearing altogether [86]. This is part of the reason why hyperspectral TIR sensing is still restricted to laboratory, ground and occasional airborne measurements, e.g. [79, 86, 87].

High-end thermal sensors are typically equipped with quantum detectors to achieve short response times and very high sensitivities. These require an external cooling system that makes them bulky and expensive and significantly limits their application to airborne and satellite missions. The development of sensors based on thermal detectors that do not require cooling has allowed for significant miniaturisation of thermal cameras, making such sensors sufficiently lightweight for inclusion as part of a UAV payload. However, the lack of a cooling system results in slow response time and low signal-to-noise ratio and makes such cameras sensitive to changes in environmental conditions—a significant issue highlighted by a number of studies [88–90]. The ability to detect stress can therefore not only be affected by plant physiological responses but also by the choice of an imaging sensor, with trade-offs having to be made between thermal sensitivity and spatial, spectral, and temporal resolutions.

Regional-Level Monitoring of Forest Vitality

To date, thermal responses to stressors have mostly been investigated at the regional scale owing to the spatial resolution typically achievable with satellite and airborne sensors. The systematic literature search (see Supplementary Material for details) showed that thermal metrics derived from satellite data have largely been used for fire-related stresses (Fig. 3); this was also indicated by Johnston et al. [91]. Most of the studies used LST, typically derived from MODIS (Moderate Resolution Imaging Spectroradiometer) [92, 93] or NOAA-AVHRR (National Oceanic and Atmospheric Administration-Advanced Very High Resolution Radiometer) sensors [94], which proved valuable for mapping areas where forest fires occurred, and for early fire warning by capturing dryness, or drought stress, of forests [94–96]. Similar to forest fire mapping where the loss of foliage leads to an increase in canopy temperature, LST has additionally been used to map defoliation caused by insect outbreaks [68, 97, 98]; Abdullah et al. [97] even found canopy temperature increase to be more sensitive to subtle canopy changes caused by bark beetle defoliation than standard vegetation indices.

A large proportion of the identified satellite-based studies used thermal information to capture the extent and severity of droughts on forests, largely focusing on the analysis of LST time series, either directly or through the use of Temperature Condition Index (TCI) that normalises LST relative to historical minimum and maximum values. In many cases, large-scale analyses were performed, comparing responses of different land cover types and broadly defined forest types (deciduous vs. evergreen and/or broadleaf vs. needleleaf) to drought onsets [100–102]. The effects of well-known climate extreme events such as El Niño were also frequently evaluated in the Amazon [103, 104]. Few studies were undertaken in temperate study areas, where LST proved to be a useful predictor of drought [105] or the water status [106] in a range of tree species. In the study of Mildrexler et al. [105], it was used in combination with a water balance to assess vulnerability of different forest types in Oregon and Washington, USA.

Table 1 Currently operational and planned (being developed or proposed) LWIR TIR satellite missions for land surface applications, alongside airborne and UAV-borne sensors utilised by previous studies for stress detection in forests. The airborne and UAV-borne entries are illustrative of current capabilities rather than being an exhaustive list of available solutions

	Agency/manufacturer	Instrument	Platform	No. bands	Spectral range	Spatial resolution
Satellite operational	NOAA	ABI	GOES-16/17/18	7	7.24–13.6 µm	2000 m
	NOAA, NASA	VIIRS	JPSS-1, JPSS-2	4	8.55–12.01 µm	750 m
	EUMETSAT, NOAA	AVHRR3	NOAA-19/B/C	2	10.3–12.5 µm	1100 m
	METI, NASA	ASTER	Terra	5	8.12–11.65 µm	90 m
	USGS, NASA	ETM +	Landsat 7	1	10.4–12.5 µm	60 m
	USGS, NASA	TIRS	Landsat 8	2	10.5–12 µm	100 m
	USGS, NASA	TIRS-2	Landsat 9	2	10.5–12 µm	100 m
	NASA	MODIS	Terra, Aqua	8	8.4–14.38 µm	1000 m
	NASA	PHyTIR	ECOSTRESS	1	8–12.5 µm	60 m
	ESA, COM	SLSTR	Sentinel-3A/3B	2	10.85–12 µm	1000 m
	ESA, NSO	HyperScout-2	PhiSat-1	4	8–14 um	390 m
	JMA	AHI	Himawari-8/9	7	7.3–13.28 µm	2000 m
	JAXA	CIRC	ALOS-2	1	8–12 µm	210 m
	JAXA	SGLI	GCOM-C	1	10.8–12 µm	1000 m
	CAST	IRMSS-2 (HJ-2)	HJ-2A/2B	1	10.5–12.5 µm	300 m
	Roscosmos	MSU-IK-SR	Kanopus-V-IR N2	1	8.4–9.4 µm	200 m
	Roshydromet, Roscosmos	MSU-MR	Meteor-M N2-2	2	10.5–12.5 µm	1000 m
Satellite planned	COM	LSTR	Sentinel LSTM-A/B	5	8.42–12.47 µm	50 m
	USGS, NASA	LandIS	Landsat-Next	5	8.3–12 µm	60 m
	NASA, ASI	SBG TIR Instrument	SBG-TIR	8	tbd	tbd
	CSA, NRCAN, ECCC	CWFMS	WildFireSat	1	10.4–12.3 µm	400 m
	Roshydromet	Advanced MSU-MR	Meteor-MP N1/2/3	2	10.5–12.5 µm	1000 m
	Roscosmos	BIK-SD 1	Resurs-PM N1/2/3	5	8.1–12.5 µm	20 m
Airborne	SPECIM	AisaOWL	Dornier 228 [65]	96	7.7–12.3 µm	2 m @ 1300 m
	NASA	MASTER	Undefined aircraft [66]	25	3.1–12.9 µm	35 m
	Space Instruments	FireMapperTM 2.0	King Air A100 [67]	1	8–12.5 µm	2.2 m @ 1160 m
	Optech	CM-LW640	Undefined aircraft [68]	1	8–14 µm	1 m @ 2000 m
	InfraTec GmbH	ImageIR 9400	Vulcanair P-68 Observer 2 [69]	1	3.6–4.9 µm	1 m @ 1270 m
	InfraTec GmbH	VarioCam	Undefined helicopter [38]	1	7.5–14 µm	0.2 m @ 130 m
	FLIR	SC655	Cessna aircraft [70]	1	7.5–14 µm	0.6 m @ 350 m
UAV-borne	FLIR	TAU 2	RotorKonzept RK-8x [71], Mikrokopter OktoXL [72]	1	7.5–13 µm	0.15 m @ 120 m
	FLIR	SC305	Aerialtronics Altura AT8 [73], VulcanUAV [73]	1	7.5–13 µm	0.17 m @ 90 m

Table 1 (continued)

Agency/manufacturer	Instrument	Platform	No. bands	Spectral range	Spatial resolution
Optris	PI450	QuestUAV Qpod [74], DJI Phantom 4 [75]	1	7.5–13 µm	0.15 m @ 60 m
DJI	M2ED	DJI Mavic 2 [76]	1	8–14 µm	0.03 m @ 60 m
senseFly	thermoMAP	Sensefly eBee [77]	1	7.5–13 µm	0.25 m @ 90 m

Despite the relatively broad use of satellite-derived thermal metrics that have proven valuable for monitoring drought, the link with tree physiology (e.g. tree radial growth) remains underexplored. Several studies using satellite-derived vegetation indices (e.g. NDVI) were able to capture physical damage on trees, but indicated that more subtle stresses, such as drought stress, were difficult to capture and only possible when leaf discoloration occurred, e.g. due to a heatwave [107, 108]. At airborne level, investigations into drought responses in the thermal domain have so far largely focused on intercomparisons. Pierce et al. [109] observed that whilst large differences in relative leaf water content clearly exhibited themselves in thermal imagery of needleleaf plots, smaller differences were not discernible at that scale. Scherrer et al. [38] similarly observed canopy temperature readings in 'dry' and 'moist' forest sites to diverge during drought onset, with responses differing between species, though these could not be attributed to the measured differences in sap flow. With rapidly evolving sensors with higher spatial, temporal, and spectral resolutions, opportunities are now opening to perform such investigations with satellite-derived thermal indices and to link them to field observations to study species-specific drought responses, detect droughts, and establish their effects on tree growth.

Local-Level Investigations with UAV Thermography

UAVs equipped with miniaturised sensors are often praised for their flexibility of deployment and ability to capture a very high level of spatial detail (Table 1), offering the chance to individually measure dominant trees. A growing number of studies have demonstrated the potential of different UAV sensors for vegetation surveys, with applications including extraction of structural parameters [110, 111], species classification [112, 113], health monitoring [114, 115], phenology tracking [116, 117], and mapping of flowering resources [118, 119]. In the case of UAV thermography, capabilities are being extensively explored for precision agriculture applications to aid early stress detection and irrigation scheduling, with a broad range of studies successfully relating canopy temperature with stress intensity in both non-woody crops [22, 120, 121] and orchard trees [18–21]. In contrast, the uptake in forestry has so far been minimal; we identified only 8 research publications, which utilised UAV-borne thermal cameras to investigate stress responses in a forest setting (Fig. 4) [71–75, 77, 122, 123]. These generally made relative temperature comparisons, finding more stressed trees to have higher canopy temperatures.

The investigated stress agents were varied, with more emphasis on biotic stressors rather than water scarcity (Fig. 4). We associate this diversity with the ability to investigate thermal responses of individual trees, which has so far been impossible to achieve (in the case of

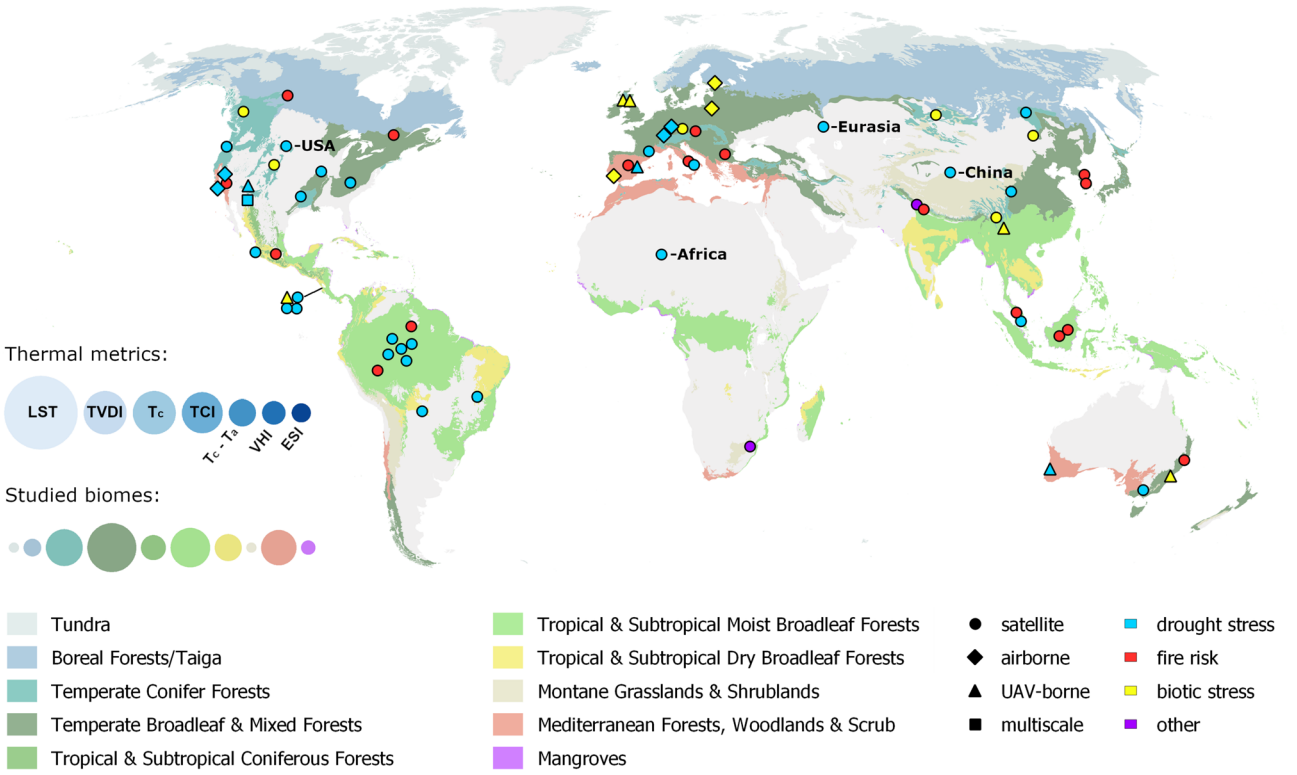

Fig. 3 Distribution of study areas from the reviewed literature ($n = 62$), categorised by the used platform (symbol) and the investigated stress agent (colour), overlain on the studied biomes. Note: several publications utilised multiple, distant study areas—these are marked separately on the map. Bubble charts present the relative frequency at which each thermal metric was used and a given biome was studied. For simplicity, TVDI encompasses other indices that combine LST and NDVI to establish non-water stressed and non-transpiring upper baselines. Abbreviations: LST Land Surface Temperature, TVDI Temperature-Vegetation Dryness Index, T_c canopy temperature, T_a air temperature, TCI Temperature Condition Index, VHI Vegetation Health Index, ESI Evaporative Stress Index. Biome extents were sourced from Dinerstein et al. [99]

satellite imagery due to spatial resolution), costly (in the case of airborne campaigns), or logistically complex (for proximal sensors). Previous airborne campaigns, which assessed defoliation induced by insect and disease outbreaks and found canopy temperature increase to be a valuable metric [69, 70], contributed to this interest.

Plant-parasite interactions have emerged as an area of interest thanks to high spatial resolution imagery enabling visual separation of individual canopies. Yuan et al. [71] found that whilst liana infestation caused a significant increase in canopy temperature, the absolute differences were small, i.e. circa 0.5 °C. Maes et al. [73], too, observed mistletoe infestation to increase canopy temperature in eucalypt. However, these differences were only significant when solar radiation was highest. Smigaj et al. [75] similarly found that canopy temperature differences between Scots pines with different red band needle blight infection rates were most pronounced when the vapour pressure deficit was highest. Weather conditions favouring increased transpiration rates accentuate these differences as stomata of the stressed plants close to prevent water loss, leading to an increase in leaf and canopy temperature. The effect of environmental conditions should, therefore, be taken into account when planning and conducting UAV-borne thermal surveys.

Beyond environmental variables, forest structure and density can impact canopy temperature and potentially obscure thermal stress responses. Wang et al. [123] found LiDAR-derived LAI

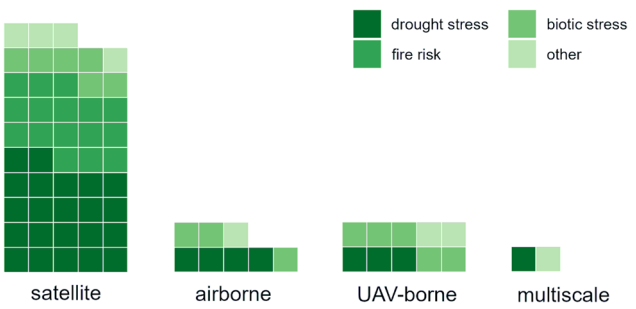

Fig. 4 Number of thermal remote sensing publications focusing on detection and assessment of stress responses in forests, categorised by topic for each remote sensing platform—every square represents a single publication. Further details on categorisations and the literature search criteria can be found in the Fig. 1 caption and in the Supplementary Material

measurements to be well correlated with canopy temperatures, impacting the relationship between canopy temperature and damage extent from a pine shoot beetle attack. Likewise, Sankey and Tatum [77] observed the impact of changing pine forest density, with trees in thinned areas consistently having significantly higher canopy temperatures even though during a severe drought the non-thinned stands experienced both lower moisture content and higher mortality rates. This discrepancy, however, was not reflected in multi-year canopy temperature measurements as the difference between a drought and a non-drought year was much higher in the non-thinned stands (9.5 °C vs. 6.9 °C), indicating higher stress levels were being experienced (compared to the non-drought baseline). Variation in differences between canopy and air temperature resulting from tree density and height was also evident in the study of Javadian et al. [76]; nevertheless, diurnal canopy temperature dynamics were closely related to tree sap flow measurements and drought stress.

This small pool of studies provides promising insights into the potential of UAV thermography, but also highlights that the interpretation of differences in canopy temperature may not be straightforward due to a range of confounding variables. Hence, development and testing of approaches that can enable direct interpretation of multitemporal thermal information of forest canopies at local scale is imperative for broader application of thermography that goes beyond relative comparisons of canopy temperatures. Proximal sensing with thermal cameras or infrared radiometers deployed on above-canopy observation towers, although not covered in depth in this review, could play an important role in helping develop these capabilities. Whilst covering very limited spatial extents, such sensors allow continuous monitoring of leaf and/or canopy temperatures, providing insight into temporal variations. As such, they could guide interpretation of UAV datasets, which only provide snapshots in time. Even though the use of such sensors still requires careful accounting for atmospheric conditions, measurement distance, and viewing angle to ensure accurate canopy temperature retrieval [50, 124], a number of studies successfully utilised them in forest habitats to characterise diurnal temperature dynamics [125–127], investigate responses to changing soil moisture conditions [54, 127], explore differences between species [33, 54, 127], and link canopy temperature measurements with gross primary productivity [128].

Open Challenges and Opportunities for Monitoring Stress Responses in Forest Ecosystems with TIR Remote Sensing

Disentangling Stress Responses from Environmental Factors

The vast majority of reviewed publications used temperature measurements directly (using LST, canopy temperature, or TCI) to identify stress (Fig. 3). In the case of satellite imagery, multitemporal analysis was often employed to identify anomalies (for the time of year) likely caused by drought onset or defoliation. Where data from a single acquisition were utilised, typically in airborne and UAV studies, relative comparisons were made between stands or trees undergoing different levels of stress or defoliation. Whilst such a direct approach would still be appropriate for comparing canopy temperatures in datasets acquired under nearly identical environmental settings, it significantly limits the use of thermal information for monitoring tree physiological status over time. The close relationship between canopy temperature and ambient environmental conditions (as mentioned in the 'Physiological responses to stress onset' section) makes it difficult to separate stress response from the effects of plant thermoregulation.

Different approaches have been developed over the years in an attempt to normalise leaf and canopy temperature for variations in environmental conditions, with the so-called 'stress indices' typically being utilised in UAV and proximal agricultural studies [3, 129, 130]. Among the most commonly used are the Crop Water Stress Index (CWSI) and canopy-to-air temperature difference ($T_c - T_a$). CWSI introduces a non-water-stressed baseline and a non-transpiring upper baseline for normalisation and was shown to robustly account for the effects of changing weather conditions [131, 132]. Several approaches for its derivation were developed, requiring a different number of additional input variables and effectively offering different levels of normalisation. A comprehensive review of these, mainly focussing on agricultural studies, alongside their limitations can be found in Maes and Steppe [3] and Nanda et al. [129]. $T_c - T_a$ is simpler to derive, requiring only ambient temperature as input, and has so far been the only thermal 'stress index' utilised in a forest setting at UAV level [75]. Although providing some level of normalisation, it was shown to be adversely affected by weather conditions, which complicates its interpretation [3].

At satellite level, several studies used a combination of LST and NDVI to help interpret the thermal responses and relate them to stress. Similarly to CWSI, a 'dry edge' representing a non-transpiring upper baseline and a 'wet edge' representing a non-water-stressed baseline can be used to normalise the responses. To derive these and subsequently the Temperature–Vegetation Dryness Index (TVDI) or similar indices, a sufficiently large study area is required to represent the entire range of surface moisture contents, from wet to dry and from bare soil to fully vegetated surfaces. Although successfully employed for studying drought across different land cover types, the TVDI uncertainty increases with NDVI values, somewhat reducing its utility to forest studies. A potential way forward could be the Evaporative Stress Index (ESI) that has been utilised by

Pascolini-Campbell et al. [133] and Yang et al. [134••] to study forest mortality rates and is now available as a product of the ECOSTRESS mission. ESI is the ratio between the potential and actual evapotranspiration and is derived with the help of a Penman–Monteith surface energy balance model; this adds complexity to its calculation and introduces the need for meteorological inputs, significantly limiting its application at local scale, but also offers a more comprehensive way of monitoring stress responses.

Further development and testing of approaches for thermal data analysis, including their applicability for different tree species and sensitivity under different climatic conditions, is required to establish how thermography can complement current forest health monitoring approaches. To date, very little research has been conducted on species-specific thermal stress responses. Addressing this gap will require direct links to be made between thermal indices and field observations of tree physiological status (e.g. measurements of sap flow, radial stem size changes, or leaf water potential) and the effects of external factors (e.g. environmental conditions or structural differences), eventually enabling direct interpretation of multitemporal thermal information of forest canopies.

Modelling Forest Thermal Properties

Surface temperature retrieval from satellite or airborne TIR data in forest environments is complicated by numerous variables that influence the thermal response. These include sun-sensor geometry, atmospheric conditions, forest density, canopy architecture, temperature, and emissivity of canopy components, as well as temperature and emissivity of soil (for open canopies). The relationship between these variables and surface temperature can be examined with Radiative Transfer Models (RTMs) that can simulate radiation propagation and scattering and the aggregated thermal response for a sample sensor. Simulations require user-specified structural, optical, and thermal properties of all vegetation scene components, as well as atmospheric profile [135–137]. RTMs can be divided into simple 1D and more complex 3D models based on how they model vegetation canopies. 1D models approximate the canopy as one or more horizontal layers of homogeneous turbid medium above a soil layer, making them unsuitable for heterogeneous sites with discontinuous canopies like forests [138–141], whereas 3D models allow the use of heterogeneous 3D scenes and therefore provide a better characterisation of forest canopies. An in-depth review of available TIR RTMs and their historical developments can be found in Cao et al. [138•].

The ability to incorporate structural complexity in simulations is the main strength of 3D RTMs. These models allow the reconstruction of realistic 3D forest scenes where canopies are represented as geometric objects (spheroid, cone, cylinder) or as detailed 3D models with explicitly defined canopy architecture down to leaf and twig level [136, 1371385). The use of realistic forest scenes was reported to improve the accuracy of simulation since vertical and horizontal heterogeneity in structure, as well as the biochemical and thermal properties of the forest canopy, could be accounted for [135, 139, 141]. Despite their superiority, 3D RTMs have three main limitations: (i) the simulations are slow and computationally demanding [142, 143]; (ii) they require the temperature of each scene component as input to simulate thermal emissions, i.e. the model can neither simulate surface sensible and latent heat fluxes; and (iii) there is no link between leaf temperature and biochemical traits [135, 138, 144], e.g. reducing leaf water content to simulate drought will not result in simulating stomatal closure and increasing leaf temperature. To address the latter, 3D RTMs can be coupled with atmosphere-soil-canopy energy balance models as demonstrated by Baldocchi and Meyers [144] and Bian et al. [139]. Though, this approach is yet to be employed in the more comprehensive 3D RTMs that explicitly define the canopy structure, such as DART (Discrete Anisotropic Radiative Transfer) [135, 145] or DIRSIG (Digital Imaging and Remote Sensing Image Generation) [146]. Another potential solution would be to utilise 3D thermal temperature point clouds derived from UAV imagery (see the '3D thermal point clouds: potential and issues' section) as inputs for 3D RTMs to define the 3D temperature distribution within each forest canopy. Though, this would require addressing occlusion issues, which hinder the estimation of lower canopy and understorey temperature. Deployment of proximal sensors in lower canopy layers could potentially help alleviate these.

The use of 3D RTMs in the TIR domain presents a promising avenue for advancing our understanding of forest thermal responses observed by coarse resolution sensors. This is due to the ability of 3D RTMs to simulate LST at the individual tree level, as a function of brightness temperature and emissivity. Of high value is their ability to separate the contribution of each scene component (leaf, wood, branches, understorey, soil) to the aggregated pixel temperature of a given sensor. Furthermore, their capability to simulate the same forest scene using multiple sensors (such as UAV-borne, airborne, and spaceborne) facilitates comparisons between simulated datasets at different levels (Fig. 5). Multiscale comparisons of thermal stress responses in forests are still scarce, with the study of Javadian et al. [76] being the only one to utilise different platforms for this purpose. Parameterisation of realistic forest 3D RTMs at sufficient spatial scale to simulate satellite-level thermal responses still poses a challenge due to the number of inputs and the required spatial extent to be modelled. Therefore, there is a need for improved understanding and prioritisation of key parameter inputs to enable more accurate and efficient

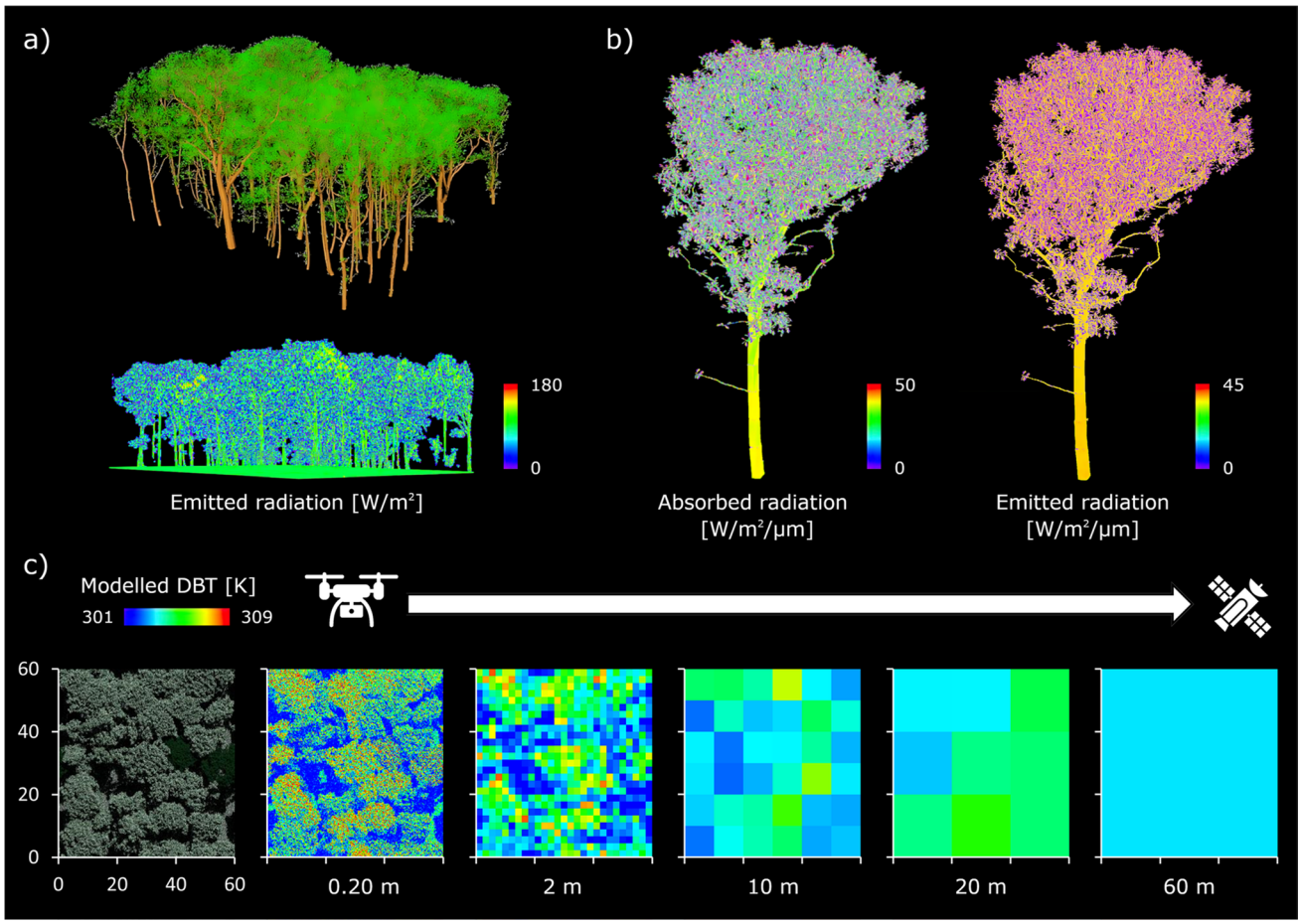

Fig. 5 **a** A mixed-species DART forest scene reconstructed from terrestrial laser scans of a forest stand in Wytham Woods, UK, that was used for a simulation of directional brightness temperature (DBT)—the 3D forest model was sourced from Calders et al. [136]. Shown alongside is a 3D radiative budget displaying the amount of TIR radiation emitted by each 0.2 m voxel within the scene. **b** A sample tree extracted from the plot showing TIR radiation absorbed and emitted by each tree component, i.e. individual leaves, branches, twigs, and the stem. **c** DBT simulated for a range of spatial resolution settings illustrating the progressive loss of spatial detail, shown next to the corresponding RGB image

upscaling of such models. In this regard, we see linking simulations with high spatial resolution measurements obtained from UAVs and proximal sensors as a promising approach.

3D Thermal Point Clouds: Potential and Issues

UAV imaging opens the opportunity to derive thermal information in three dimensions by utilising the Structure-from-Motion (SfM) workflow, potentially enabling the study of temperature variations across canopy layers. Such datasets could prove to be valuable inputs for 3D RTMs, helping define the 3D temperature distribution within each forest canopy. Whilst promising, SfM processing of thermal UAV data for forests has some specific challenges since the SfM workflow was originally developed for processing red–green–blue (RGB) imagery obtained from different viewing angles and/or orientations where unique features can be easily identified and matched. Due to the inherently low spatial resolution of thermal imagery (typically several decimetres) compared to other modalities and often subtle temperature differences within the forest canopy that are close to the accuracy of the used cameras, it is difficult to find enough corresponding points on overlapping images to reconstruct exact camera positions. This leads to problems with aligning all images and low geometrical accuracies, if stitching is possible at all. Consequently, when only thermal data is used, the SfM processing often fails at the construction of a dense point cloud, which is essential for adequate reconstruction of the surface and subsequent creation of thermal orthomosaics. Many of the reviewed UAV-borne studies faced this issue and resorted to using individual thermal images for the analysis instead [71, 75, 77, 123].

Co-registration with RGB or multispectral datasets, which have a higher spatial detail, can aid processing of the thermal data. Several methods across different application domains have been proposed to achieve this; some require the use of ground control points [147, 148], whilst others realise the alignment through post-processing of the camera positions [149] or alignment of the RGB and TIR point clouds [150]. These, however, are either cumbersome to implement or do not solve the initial alignment issues faced in forests. One way to overcome the highlighted problems and avoid the complicated alignment procedures is to co-acquire thermal data with coincident high-resolution datasets, such as RGB or multispectral data, and use the fused dataset for photogrammetric processing, building up on the methodology proposed by Ham and Golparvar-Fard [151]. An example result of such processing is shown in Fig. 6, for which a FLIR Tau 2 thermal camera attached to and synchronised with an Airphen multispectral camera was used. Both the RGB and TIR point clouds were generated in SfM software, though the workflow did not follow the standard SfM protocol. Instead, the focus was first put on the reconstruction of reliable geometry, for which all images taken by all multispectral cameras and the TIR camera were loaded together and co-registered through SfM, followed by the generation of a dense point cloud. Only then the responses from different cameras were separated and calibrated, and temperature values assigned in the 3D space to the previously generated dense point cloud (Fig. 6). This approach overcomes difficulties with aligning thermal images in forest environments, such as those experienced by Webster et al. [152], and results in a good co-registration of multispectral and TIR SfM products. The use of TIR data together with RGB or multispectral data in the co-registration procedure also bypasses several steps applied by Javadnejad et al. [153] where the TIR images are only added to the SfM process at a later stage and are thus not directly aligned. Such optimisation of the processing workflow is crucial for the effective use of UAV thermography.

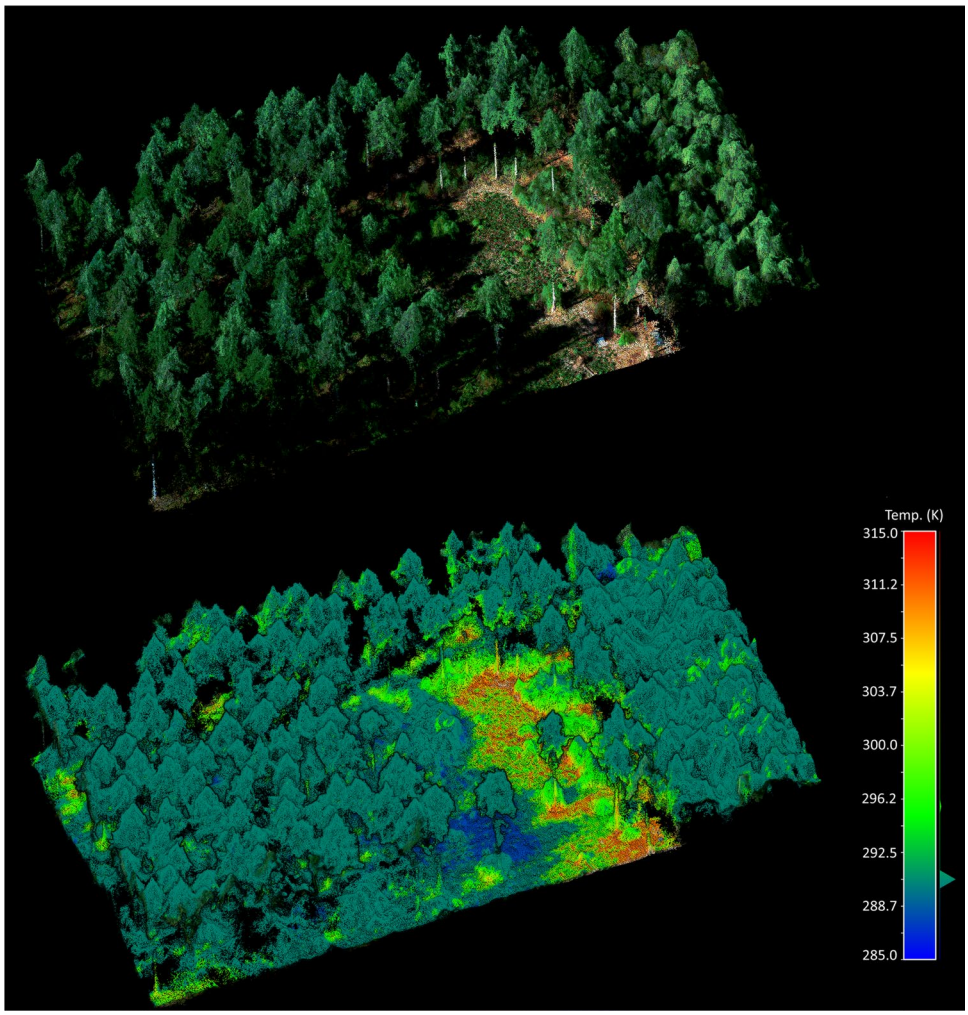

Fig. 6 RGB and TIR point clouds of a Douglas fir forest stand in the Zwolse Bos, the Netherlands. The colours in the TIR point cloud show the temperature in Kelvin degrees

Quality of UAV-Borne Thermal Imagery

The quality of thermal data obtained from UAV platforms is strongly impacted by the performance of available miniature cameras. Even though manufacturers often claim temperature reading accuracy to be within 2 °C or 2%, the actual offsets can be much larger, especially if environmental conditions are changing. This is due to the way thermal detectors operate; as they absorb IR radiation emitted from an observed surface, the amount of produced heat varies, leading to a change in the electrical properties of the detectors and consequently in the recorded image pixel values. Varying camera body temperature caused by changing ambient conditions will, therefore, also affect the detectors. In particular, rapid increases in camera body temperature caused by external heat were shown to strongly affect temperature readings in uncooled cameras [89, 90, 154]. Ensuring a camera has sufficient time to adjust to ambient conditions prior to the acquisition, and limiting the sun's influence during the acquisition, e.g. through shielding, can help with obtaining more consistent temperature measurements over time. Similarly, ensuring a camera is turned on for a sufficient time prior to the flight is crucial because significant thermal drift occurs during the warming up period—previous studies suggested a waiting time between 30 and 60 min is needed for miniature uncooled cameras to stabilise [88–90, 147].

Even with these precautions in place, some thermal drift is likely to occur and may need to be accounted for to ensure that the observed canopy temperature differences reflect reality. This can, for example, be achieved through the comparison of temperatures recorded for the same areas in overlapping images [155]—a feature already available in some software implementing the SfM workflow. Alternatively, the use of an external heated shutter mounted on the camera for mid-flight calibration has been suggested for alleviating thermal drift [156]. Atmospheric conditions and the measurement distance will also have an effect on recorded temperature values, dictating the extent to which the thermal signal gets attenuated, with the most significant atmospheric factors being relative humidity and atmospheric temperature. Where absolute temperature values are needed (i.e. for analysis beyond comparison of relative canopy temperature differences), further corrections with the help of ground measurements are required. A common approach in agricultural studies is to utilise a range of targets on the ground (ideally including targets that are hotter and colder than plant canopies) and relate their temperatures, as measured on the ground, to temperatures recorded by the camera; this has for example been applied by Egea et al. [20], Messina and Modica [130], and Gómez-Candón et al. [157], achieving varying levels of accuracy. Further research is, therefore, required to develop robust UAV thermal data collection strategies, bearing in mind the challenges of sensor calibration, measurement uncertainties, and temporal stability of acquired information.

Exploration into Spectral Emissivity

Whilst thermography is conventionally used for detecting early signs of stress through observation of leaf and canopy temperatures, it contains further information that can potentially be exploited. Spectral variations in emissivity can reveal useful absorption features, much like in the VIS-SWIR spectra. Hyperspectral TIR remote sensing has so far been mostly explored in geology for mapping of mineralogy and lithology since a wide range of minerals have strong absorption and emission bands in the LWIR spectral range [158–161]. In plant sciences, little attention has been given to it thus far, largely due to the need for specialised instruments that are capable of capturing TIR spectral features of plants.

A number of laboratory studies on different plant types have shown that spectral emissivity differs between species and indicated that spectra are strongly affected by the leaf surface composition since penetration of energy into leaf surfaces is limited in the TIR region [79, 86, 162, 163]. Only recently, the first investigations into the effects of stress on leaf spectral emissivity have been performed, revealing species-specific responses following exposure to stress [164–166]. These were generally attributed to biochemical and structural changes occurring in the leaf in response to stress. For example, Buitrago et al. [164] and Gerhards et al. [165] suggested that increases in emissivity they observed were related to an increased thickness of the cuticle, which caused a cavity effect, i.e. a loss of spectral contrast and an increase in emissivity value that occurs due to multiple surface scattering [167]. This change in spectral emissivity was found by Gerhards et al. [165] to be more sensitive to drought stress onset in potato plants than VNIR and SWIR vegetation indices.

Although a promising development, further research is required to better understand: (i) how strategies for coping with stress affect leaf spectral emissivity in different species, (ii) what effects different biotic and abiotic stress agents have, and (iii) what levels of stress are discernible in TIR spectra. Further canopy-level studies are required to assess how distinctive are the stress responses in canopy spectral emissivity. Meerdink et al. [79] found that whilst a good proportion of tree species they investigated were spectrally separable at leaf level, species mapping was no longer possible using airborne data due to significant overlaps in TIR spectral responses at canopy level. Ribeiro da Luz and Crowley [163] similarly found that canopy geometry and composition affected spectral emissivity and separability of different tree species. Improvements in sensor field of view, signal-to-noise ratio, and data analysis methods, especially those

linking leaf and canopy TIR spectral responses, are therefore needed to explore the potential of spectral emissivity.

Conclusions and Outlook for the Future

Monitoring of leaf and canopy temperature can provide valuable information on tree physiological status. However, the influences of environmental factors and structural composition pose a challenge for the direct interpretation of thermal data. Further development and testing of data analysis approaches, including their applicability for different tree species and sensitivity under different climatic conditions, is required to establish how thermal remote sensing can best complement current forest health monitoring approaches. This will require direct links to be made with tree physiological status and the effects of external factors (e.g. environmental conditions or structural differences). In this regard, we foresee UAV thermography as playing an increasingly important role, allowing individual tree analysis and derivation of thermal information in three dimensions. The use of radiative transfer models could help address some of the challenges related to variation in leaf structural traits and canopy architecture and allow scaling responses to forest stand level, though further model developments are still required to make this link possible.

The launch of new satellite missions delivering high spatio-temporal resolution data, such as Sentinel LSTM and Landsat Next, will open new possibilities for close monitoring of the variability in LST and, hence, in evapotranspiration. However, full realisation of the TIR data potential for forest health monitoring will require multimodal approaches that allow distinct stress responses to be investigated. Whilst a number of studies have successfully combined hyperspectral/multispectral sensing with LiDAR metrics [168–170], the integration of these modalities with TIR data in forest environments for stress detection remains relatively unexplored despite promising outcomes in the agricultural domain [171]. Although not discussed in detail here, we recommend such a synergistic approach to both improve the understanding of structural effects on the thermal stress responses and provide a more holistic overview of forest condition.

Supplementary Information The online version contains supplementary material available at https://doi.org/10.1007/s40725-023-00207-z.

Author contributions M.S. conceptualised the review, designed and undertook the systematic literature search, and led the writing of the manuscript with contributions from A.A., H.B., M.D., A.E. and A.J. Visualisations were prepared by M.S. (Figs. 1, 2, 3, 4 and 5), A.A. (Fig. 2), H.B. (Fig. 6) and A.E. (Fig. 5). All authors critically reviewed the manuscript and agreed to the published version.

Declarations

Conflict of Interest The authors declare no conflict of interest.

Human and Animal Rights and Informed Consent This article does not contain any studies with human or animal subjects performed by any of the authors.

References

Papers of particular interest, published recently, have been highlighted as:
- • Of importance
- •• Of major importance

1. Leinonen I, Grant OM, Tagliavia CPP, Chaves MM, Jones HG. Estimating stomatal conductance with thermal imagery. Plant, Cell Environ. 2006;29(8):1508–18. https://doi.org/10.1111/j.1365-3040.2006.01528.x.
2. Grant OM, Chaves MM, Jones HG. Optimizing thermal imaging as a technique for detecting stomatal closure induced by drought stress under greenhouse conditions. Physiol Plant. 2006;127(3):507–18. https://doi.org/10.1111/j.1399-3054.2006.00686.x.
3. Maes WH, Steppe K. Estimating evapotranspiration and drought stress with ground-based thermal remote sensing in agriculture: a review. J Exp Bot. 2012;63(13):4671–712. https://doi.org/10.1093/jxb/ers165.
4. Lima RSN, García-Tejero I, Lopes TS, Costa JM, Vaz M, Durán-Zuazo VH, et al. Linking thermal imaging to physiological indicators in Carica papaya L. under different watering regimes. Agricult Water Manag. 2016;164:148–57. https://doi.org/10.1016/j.agwat.2015.07.017.
5. Chaerle L, Hagenbeek D, De Bruyne E, Van Der Straeten D. Chlorophyll fluorescence imaging for disease-resistance screening of sugar beet. Plant Cell, Tissue Organ Cult. 2007;91(2):97–106. https://doi.org/10.1007/s11240-007-9282-8.
6. Oerke EC, Fröhling P, Steiner U. Thermographic assessment of scab disease on apple leaves. Precision Agric. 2011;12(5):699–715. https://doi.org/10.1007/s11119-010-9212-3.
7. Jafari M, Minaei S, Safaie N. Detection of pre-symptomatic rose powdery-mildew and gray-mold diseases based on thermal vision. Infrared Phys Technol. 2017;85:170–83. https://doi.org/10.1016/j.infrared.2017.04.023.
8. Wen D-M, Chen M-X, Zhao L, Ji T, Li M, Yang X-T. Use of thermal imaging and Fourier transform infrared spectroscopy for the pre-symptomatic detection of cucumber downy mildew.

Eur J Plant Pathol. 2019;155(2):405–16. https://doi.org/10.1007/s10658-019-01775-2.
9. Bandeen WR, Hanel RA, Licht J, Stampfl RA, Stroud WG. Infrared and reflected solar radiation measurements from the Tiros II meteorological satellite. J Geophys Res (1896-1977). 1961;66(10):3169–85. https://doi.org/10.1029/JZ066i010p03169.
10. Hua L, Shao G. The progress of operational forest fire monitoring with infrared remote sensing. J For Res. 2017;28(2):215–29. https://doi.org/10.1007/s11676-016-0361-8.
11. Wooster MJ, Roberts G, Smith AMS, Johnston J, Freeborn P, Amici S, et al. Thermal remote sensing of active vegetation fires and biomass burning events. In: Kuenzer C, Dech S, editors., et al., Thermal infrared remote sensing: sensors, methods, applications. Dordrecht: Springer, Netherlands; 2013. p. 347–90. https://doi.org/10.1007/978-94-007-6639-6_18.
12. Leblon B, San-Miguel-Ayanz J, Bourgeau-Chavez L, Kong M. 3 - Remote Sensing of Wildfires. In: Land surface remote sensing: Elsevier. 2016. p. 55–95.
13. Schroeder W, Oliva P, Giglio L, Csiszar IA. The New VIIRS 375m active fire detection data product: algorithm description and initial assessment. Remote Sens Environ. 2014;143:85–96. https://doi.org/10.1016/j.rse.2013.12.008.
14. Schroeder W, Prins E, Giglio L, Csiszar I, Schmidt C, Morisette J, et al. Validation of GOES and MODIS active fire detection products using ASTER and ETM+ data. Remote Sens Environ. 2008;112(5):2711–26. https://doi.org/10.1016/j.rse.2008.01.005.
15. Lizundia-Loiola J, Otón G, Ramo R, Chuvieco E. A spatio-temporal active-fire clustering approach for global burned area mapping at 250 m from MODIS data. Remote Sens Environ. 2020;236:111493. https://doi.org/10.1016/j.rse.2019.111493.
16. Chowdhury EH, Hassan QK. Operational perspective of remote sensing-based forest fire danger forecasting systems. ISPRS J Photogramm Remote Sens. 2015;104:224–36. https://doi.org/10.1016/j.isprsjprs.2014.03.011.
17. Szpakowski DM, Jensen JLR. A review of the applications of remote sensing in fire ecology. Remote Sensing. 2019;11(22):2638. https://doi.org/10.3390/rs11222638.
18. Berni JAJ, Zarco-Tejada PJ, Sepulcre-Cantó G, Fereres E, Villalobos F. Mapping canopy conductance and CWSI in olive orchards using high resolution thermal remote sensing imagery. Remote Sens Environ. 2009;113(11):2380–8. https://doi.org/10.1016/j.rse.2009.06.018.
19. Gonzalez-Dugo V, Zarco-Tejada P, Nicolás E, Nortes PA, Alarcón JJ, Intrigliolo DS, et al. Using high resolution UAV thermal imagery to assess the variability in the water status of five fruit tree species within a commercial orchard. Precision Agric. 2013;14(6):660–78. https://doi.org/10.1007/s11119-013-9322-9.
20. Egea G, Padilla-Díaz CM, Martinez-Guanter J, Fernández JE, Pérez-Ruiz M. Assessing a crop water stress index derived from aerial thermal imaging and infrared thermometry in super-high density olive orchards. Agric Water Manag. 2017;187:210–21. https://doi.org/10.1016/j.agwat.2017.03.030.
21. Zarco-Tejada PJ, Poblete T, Camino C, Gonzalez-Dugo V, Calderon R, Hornero A, et al. Divergent abiotic spectral pathways unravel pathogen stress signals across species. Nat Commun. 2021;12(1):6088. https://doi.org/10.1038/s41467-021-26335-3.
22. Ekinzog EK, Schlerf M, Kraft M, Werner F, Riedel A, Rock G, et al. Revisiting crop water stress index based on potato field experiments in Northern Germany. Agric Water Manag. 2022;269:107664. https://doi.org/10.1016/j.agwat.2022.107664.
23. Prashar A, Jones HG. Infra-red thermography as a high-throughput tool for field phenotyping. Agronomy. 2014;4(3):397–417. https://doi.org/10.3390/agronomy4030397.
24. Jones HG, Rotenburg E. Energy, radiation and temperature regulation in plants. Encycl: Life Sci; 2011. https://doi.org/10.1002/9780470015902.a0003199.pub2.
25. Wohl K, James WO. The energy changes associated with plant respiration. The New Phytologist. 1942;41(4):230–56. http://www.jstor.org/stable/2428730
26. Demmig-Adams B, Adams WW III. Photoprotection in an ecological context: the remarkable complexity of thermal energy dissipation. New Phytol. 2006;172(1):11–21. https://doi.org/10.1111/j.1469-8137.2006.01835.x.
27. Ye H, Yuan Z, Zhang S. The heat and mass transfer analysis of a leaf. J Bionic Eng. 2013;10(2):170–6. https://doi.org/10.1016/S1672-6529(13)60212-7.
28. Albrecht H, Fiorani F, Pieruschka R, Müller-Linow M, Jedmowski C, Schreiber L, Schurr U, Rascher U. Quantitative Estimation of Leaf Heat Transfer Coefficients by Active Thermography at Varying Boundary Layer Conditions. Front Plant Sci. 2020;10:1684. https://doi.org/10.3389/fpls.2019.01684.
29. Caird MA, Richards JH, Donovan LA. Nighttime stomatal conductance and transpiration in C3 and C4 plants. Plant Physiol. 2007;143(1):4–10. https://doi.org/10.1104/pp.106.092940.
30. Harrison EL, Arce Cubas L, Gray JE, Hepworth C. The influence of stomatal morphology and distribution on photosynthetic gas exchange. Plant J. 2020;101(4):768–79. https://doi.org/10.1111/tpj.14560.
31. Schuepp PH. Tansley Review No. 59 Leaf boundary layers. New Phytologist. 1993;125(3):477–507. https://doi.org/10.1111/j.1469-8137.1993.tb03898.x.
32. Leigh A, Sevanto S, Close JD, Nicotra AB. The influence of leaf size and shape on leaf thermal dynamics: does theory hold up under natural conditions? Plant, Cell Environ. 2017;40(2):237–48. https://doi.org/10.1111/pce.12857.
33. Leuzinger S, Körner C. Tree species diversity affects canopy leaf temperatures in a mature temperate forest. Agric For Meteorol. 2007;146(1):29–37. https://doi.org/10.1016/j.agrformet.2007.05.007.
34. Reinert S, Bögelein R, Thomas FM. Use of thermal imaging to determine leaf conductance along a canopy gradient in European beech (Fagus sylvatica). Tree Physiol. 2012;32(3):294–302. https://doi.org/10.1093/treephys/tps017.
35. Sack L, Melcher PJ, Liu WH, Middleton E, Pardee T. How strong is intracanopy leaf plasticity in temperate deciduous trees? Am J Bot. 2006;93(6):829–39. https://doi.org/10.3732/ajb.93.6.829.
36. Finnigan JJ, Shaw RH, Patton EG. Turbulence structure above a vegetation canopy. J Fluid Mech. 2009;637:387–424. https://doi.org/10.1017/S0022112009990589.
37. Henrion W, Tributsch H. Optical solar energy adaptations and radiative temperature control of green leaves and tree barks. Sol Energy Mater Sol Cells. 2009;93(1):98–107. https://doi.org/10.1016/j.solmat.2008.08.009.
38. Scherrer D, Bader MK-F, Körner C. Drought-sensitivity ranking of deciduous tree species based on thermal imaging of forest canopies. Agric For Meteorol. 2011;151(12):1632–40. https://doi.org/10.1016/j.agrformet.2011.06.019.
39. Costa JM, Grant OM, Chaves MM. Thermography to explore plant–environment interactions. J Exp Bot. 2013;64(13):3937–49. https://doi.org/10.1093/jxb/ert029.
40. Still C, Powell R, Aubrecht D, Kim Y, Helliker B, Roberts D, et al. Thermal imaging in plant and ecosystem ecology: applications and challenges. Ecosphere. 2019;10(6):e02768. https://doi.org/10.1002/ecs2.2768. **This review gives further information on tree and ecosystem thermal regimes and their functional consequences.**
41. Thomson SJ, Ouellet-Plamondon CM, DeFauw SL, Huang Y, Fisher DK, English PJ. Potential and challenges in use of thermal

imaging for humid region irrigation system management. J Agric Sci. 2012;4:103. https://doi.org/10.5539/jas.v4n4p103.
42. Zhang J-L, Zhu J-J, Cao K-F. Seasonal variation in photosynthesis in six woody species with different leaf phenology in a valley savanna in southwestern China. Trees. 2007;21(6):631–43. https://doi.org/10.1007/s00468-007-0156-9.
43. Zhao Y, Gao J, Im Kim J, Chen K, Bressan RA, Zhu J-K. Control of plant water use by ABA induction of senescence and dormancy: an overlooked lesson from evolution. Plant Cell Physiol. 2017;58(8):1319–27. https://doi.org/10.1093/pcp/pcx086.
44. Kumar M, Kesawat MS, Ali A, Lee S-C, Gill SS, Kim HU. Integration of abscisic acid signaling with other signaling pathways in plant stress responses and development. Plants. 2019;8(12):592. https://doi.org/10.3390/plants8120592.
45. Attia Z, Domec J-C, Oren R, Way DA, Moshelion M. Growth and physiological responses of isohydric and anisohydric poplars to drought. J Exp Bot. 2015;66(14):4373–81. https://doi.org/10.1093/jxb/erv195.
46. Bennett AC, McDowell NG, Allen CD, Anderson-Teixeira KJ. Larger trees suffer most during drought in forests worldwide. Nature Plants. 2015;1(10):15139. https://doi.org/10.1038/nplants.2015.139.
47. McDowell NG, Sapes G, Pivovaroff A, Adams HD, Allen CD, Anderegg WRL, et al. Mechanisms of woody-plant mortality under rising drought, CO2 and vapour pressure deficit. Nat Rev Earth Environ. 2022;3(5):294–308. https://doi.org/10.1038/s43017-022-00272-1.
48. McGregor IR, Helcoski R, Kunert N, Tepley AJ, Gonzalez-Akre EB, Herrmann V, et al. Tree height and leaf drought tolerance traits shape growth responses across droughts in a temperate broadleaf forest. New Phytol. 2021;231(2):601–16. https://doi.org/10.1111/nph.16996.
49. Way DA, Holly C, Bruhn D, Ball MC, Atkin OK. Diurnal and seasonal variation in light and dark respiration in field-grown Eucalyptus pauciflora. Tree Physiol. 2015;35(8):840–9. https://doi.org/10.1093/treephys/tpv065.
50. Kim Y, Still CJ, Roberts DA, Goulden ML. Thermal infrared imaging of conifer leaf temperatures: comparison to thermocouple measurements and assessment of environmental influences. Agric For Meteorol. 2018;248:361–71. https://doi.org/10.1016/j.agrformet.2017.10.010.
51. Tay Zar Myo S, Zhang Y, Song Q, Deng Y, Fei X, Zhou R, et al. Analysis of canopy temperature depression between tropical rainforest and rubber plantation in Southwest China. iForest Biogeosci For. 2019;12(6):518–26. https://doi.org/10.3832/ifor3101-012.
52. Guo Z, Zhang K, Lin H, Majcher BM, Lee CKF, Still CJ, et al. Plant canopies exhibit stronger thermoregulation capability at the seasonal than diurnal timescales. Agric For Meteorol. 2023;339:109582. https://doi.org/10.1016/j.agrformet.2023.109582.
53. Habibi F, Liu T, Shahid MA, Schaffer B, Sarkhosh A. Physiological, biochemical, and molecular responses of fruit trees to root zone hypoxia. Environ Exp Bot. 2023;206:105179. https://doi.org/10.1016/j.envexpbot.2022.105179.
54. Yi K, Smith JW, Jablonski AD, Tatham EA, Scanlon TM, Lerdau MT, et al. High heterogeneity in canopy temperature among co-occurring tree species in a temperate forest. J Geophys Res: Biogeosci. 2020;125(12):e2020JG005892. https://doi.org/10.1029/2020JG005892.
55. Roelfsema MRG, Hedrich R. In the light of stomatal opening: new insights into 'the Watergate.' New Phytol. 2005;167(3):665–91. https://doi.org/10.1111/j.1469-8137.2005.01460.x.
56. Daley MJ, Phillips NG. Interspecific variation in nighttime transpiration and stomatal conductance in a mixed New England deciduous forest. Tree Physiol. 2006;26(4):411–9. https://doi.org/10.1093/treephys/26.4.411.
57. Lin H, Chen Y, Zhang H, Fu P, Fan Z. Stronger cooling effects of transpiration and leaf physical traits of plants from a hot dry habitat than from a hot wet habitat. Funct Ecol. 2017;31(12):2202–11. https://doi.org/10.1111/1365-2435.12923.
58. Zhang S, Gao R. Diurnal changes of gas exchange, chlorophyll fluorescence, and stomatal aperture of hybrid poplar clones subjected to midday light stress. Photosynthetica. 1999;37(14):559–71. https://doi.org/10.1023/a:1007119524389.
59. Urban J, Ingwers M, McGuire MA, Teskey RO. Stomatal conductance increases with rising temperature. Plant Signal Behav. 2017;12(8):e1356534. https://doi.org/10.1080/15592324.2017.1356534.
60. Reynolds-Henne CE, Langenegger A, Mani J, Schenk N, Zumsteg A, Feller U. Interactions between temperature, drought and stomatal opening in legumes. Environ Exp Bot. 2010;68(1):37–43. https://doi.org/10.1016/j.envexpbot.2009.11.002.
61. Rodríguez-Gamir J, Ancillo G, González-Mas MC, Primo-Millo E, Iglesias DJ, Forner-Giner MA. Root signalling and modulation of stomatal closure in flooded citrus seedlings. Plant Physiol Biochem. 2011;49(6):636–45. https://doi.org/10.1016/j.plaphy.2011.03.003.
62. Wilkinson S, Clephan AL, Davies WJ. Rapid low temperature-induced stomatal closure occurs in cold-tolerant Commelina communis leaves but not in cold-sensitive tobacco leaves, via a mechanism that involves apoplastic calcium but not abscisic acid. Plant Physiol. 2001;126(4):1566–78. https://doi.org/10.1104/pp.126.4.1566.
63. Pineda M, Barón M, Pérez-Bueno M-L. Thermal imaging for plant stress detection and phenotyping. Remote Sensing. 2021;13(1):68. https://doi.org/10.3390/rs13010068.
64. Mohamed HI, El-Shazly HH, Badr A. Role of salicylic acid in biotic and abiotic stress tolerance in plants. In: Lone R, Shuab R, Kamili AN. Plant phenolics in sustainable agriculture : Volume 1. Singapore: Springer Singapore. 2020. p. 533–54. https://doi.org/10.1007/978-981-15-4890-1_23.
65. NERC ARSF. ARSF 2014_219b - GB14_04 Flight. 2014. https://data.ceda.ac.uk/neodc/arsf/2014/GB14_04.
66. Coates AR, Dennison PE, Roberts DA, Roth KL. Monitoring the impacts of severe drought on southern California chaparral species using hyperspectral and thermal infrared imagery. Remote Sensing. 2015;7(11):14276–91. https://doi.org/10.3390/rs71114276.
67. Grulke N, Maxfield J, Riggan P, Schrader-Patton C. Pre-emptive detection of mature pine drought stress using multispectral aerial imagery. Remote Sensing. 2020;12(14):2338. https://doi.org/10.3390/rs12142338.
68. Junttila S, Vastaranta M, Hämäläinen J, Latva-käyrä P, Holopainen M, Hernández Clemente R, et al. Effect of forest structure and health on the relative surface temperature captured by airborne thermal imagery – case study in Norway Spruce-dominated stands in Southern Finland. Scand J For Res. 2017;32(2):154–65. https://doi.org/10.1080/02827581.2016.1207800.
69. Zakrzewska A, Kopeć D. Remote sensing of bark beetle damage in Norway spruce individual tree canopies using thermal infrared and airborne laser scanning data fusion. For Ecosyst. 2022;9:100068. https://doi.org/10.1016/j.fecs.2022.100068.
70. Hornero A, Zarco-Tejada PJ, Quero JL, North PRJ, Ruiz-Gómez FJ, Sánchez-Cuesta R, et al. Modelling hyperspectral- and thermal-based plant traits for the early detection of Phytophthora-induced symptoms in oak decline. Remote Sens Environ. 2021;263:112570. https://doi.org/10.1016/j.rse.2021.112570.
71. Yuan X, Laakso K, Marzahn P, Sanchez-Azofeifa GA. Canopy Temperature differences between Liana-infested and

non-Liana infested areas in a neotropical dry forest. Forests. 2019;10(10):890. https://doi.org/10.3390/f10100890.
72. Santini F, Kefauver SC, Resco de Dios V, Araus JL, Voltas J. Using unmanned aerial vehicle-based multispectral, RGB and thermal imagery for phenotyping of forest genetic trials: a case study in Pinus halepensis. Ann Appl Biol. 2019;174(2):262–76. https://doi.org/10.1111/aab.12484.
73. Maes WH, Huete AR, Avino M, Boer MM, Dehaan R, Pendall E, et al. Can UAV-based infrared thermography be used to study plant-parasite interactions between mistletoe and eucalypt trees? Remote Sensing. 2018;10(12):2062. https://doi.org/10.3390/rs10122062.
74. Smigaj M, Gaulton R, Barr SL, Suárez JC. UAV-borne thermal imaging for forest health monitoring: detection of disease-induced canopy temperature increase. Int Arch Photogramm Remote Sens Spatial Inf Sci. 2015;XL-3/W3:349-54. 10.5194/isprsarchives-XL-3-W3-349-2015
75. Smigaj M, Gaulton R, Suárez JC, Barr SL. Canopy temperature from an Unmanned Aerial Vehicle as an indicator of tree stress associated with red band needle blight severity. For Ecol Manage. 2019;433:699–708. https://doi.org/10.1016/j.foreco.2018.11.032.
76. Javadian M, Smith WK, Lee K, Knowles JF, Scott RL, Fisher JB, et al. Canopy temperature is regulated by ecosystem structural traits and captures the ecohydrologic dynamics of a semiarid mixed conifer forest site. J Geophys Res: Biogeoscie. 2022;127(2):e2021JG006617. https://doi.org/10.1029/2021JG006617.
77. Sankey T, Tatum J. Thinning increases forest resiliency during unprecedented drought. Sci Rep. 2022;12(1):9041. https://doi.org/10.1038/s41598-022-12982-z.
78. Rock G, Gerhards M, Schlerf M, Hecker C, Udelhoven T. Plant species discrimination using emissive thermal infrared imaging spectroscopy. Int J Appl Earth Obs Geoinf. 2016;53:16–26. https://doi.org/10.1016/j.jag.2016.08.005.
79. Meerdink S, Roberts D, Hulley G, Gader P, Pisek J, Adamson K, et al. Plant species' spectral emissivity and temperature using the hyperspectral thermal emission spectrometer (HyTES) sensor. Remote Sens Environ. 2019;224:421–35. https://doi.org/10.1016/j.rse.2019.02.009.
80. Richardson AD, Aubrecht DM, Basler D, Hufkens K, Muir CD, Hanssen L. Developmental changes in the reflectance spectra of temperate deciduous tree leaves and implications for thermal emissivity and leaf temperature. New Phytol. 2021;229(2):791–804. https://doi.org/10.1111/nph.16909.
81. Meerdink SK, Hook SJ, Roberts DA, Abbott EA. The ECOSTRESS spectral library version 10. Remote Sens Environ. 2019;230:111196. https://doi.org/10.1016/j.rse.2019.05.015.
82. Gillespie A, Rokugawa S, Matsunaga T, Cothern JS, Hook S, Kahle AB. A temperature and emissivity separation algorithm for Advanced Spaceborne Thermal Emission and Reflection Radiometer (ASTER) images. IEEE Trans Geosci Remote Sens. 1998;36(4):1113–26. https://doi.org/10.1109/36.700995.
83. Li Z-L, Tang B-H, Wu H, Ren H, Yan G, Wan Z, et al. Satellite-derived land surface temperature: current status and perspectives. Remote Sens Environ. 2013;131:14–37. https://doi.org/10.1016/j.rse.2012.12.008.
84. Borel C. Error analysis for a temperature and emissivity retrieval algorithm for hyperspectral imaging data. Int J Remote Sens. 2008;29(17–18):5029–45. https://doi.org/10.1080/01431160802036540.
85. Jacob F, Lesaignoux A, Olioso A, Weiss M, Caillault K, Jacquemoud S, et al. Reassessment of the temperature-emissivity separation from multispectral thermal infrared data: introducing the impact of vegetation canopy by simulating the cavity effect with the SAIL-Thermique model. Remote Sens Environ. 2017;198:160–72. https://doi.org/10.1016/j.rse.2017.06.006.
86. Ribeiro da Luz B, Crowley JK. Spectral reflectance and emissivity features of broad leaf plants: prospects for remote sensing in the thermal infrared (8.0–14.0 μm). Remote Sens Environ. 2007;109(4):393–405. https://doi.org/10.1016/j.rse.2007.01.008.
87. Meerdink SK, Roberts DA, King JY, Roth KL, Dennison PE, Amaral CH, et al. Linking seasonal foliar traits to VSWIR-TIR spectroscopy across California ecosystems. Remote Sens Environ. 2016;186:322–38. https://doi.org/10.1016/j.rse.2016.08.003.
88. Smigaj M, Gaulton R, Suarez JC, Barr SL. Use of miniature thermal cameras for detection of physiological stress in conifers. Remote Sensing. 2017;9(9):957. https://doi.org/10.3390/rs9090957.
89. Kelly J, Kljun N, Olsson P-O, Mihai L, Liljeblad B, Weslien P, et al. Challenges and best practices for deriving temperature data from an uncalibrated UAV thermal infrared camera. Remote Sensing. 2019;11(5):567. https://doi.org/10.3390/rs11050567.
90. Wan Q, Brede B, Smigaj M, Kooistra L. Factors influencing temperature measurements from miniaturized thermal infrared (TIR) cameras: a laboratory-based approach. Sensors. 2021;21(24). https://doi.org/10.3390/s21248466.
91. Johnston MR, Andreu A, Verfaillie J, Baldocchi D, Moorcroft PR. What lies beneath: vertical temperature heterogeneity in a Mediterranean woodland savanna. Remote Sens Environ. 2022;274: 112950. https://doi.org/10.1016/j.rse.2022.112950.
92. Jurdao S, Chuvieco E, Arevalillo JM. Modelling fire ignition probability from satellite estimates of live fuel moisture content. Fire Ecology. 2012;8(1):77–97. https://doi.org/10.4996/fireecology.0801077.
93. Qin Y, Xiao X, Wigneron J-P, Ciais P, Canadell JG, Brandt M, et al. Large loss and rapid recovery of vegetation cover and aboveground biomass over forest areas in Australia during 2019–2020. Remote Sens Environ. 2022;278:113087. https://doi.org/10.1016/j.rse.2022.113087.
94. Manzo-Delgado L, Sánchez-Colón S, Álvarez R. Assessment of seasonal forest fire risk using NOAA-AVHRR: a case study in central Mexico. Int J Remote Sens. 2009;30(19):4991–5013. https://doi.org/10.1080/01431160902852796.
95. Fernandes K, Bell M, Muñoz ÁG. Combining precipitation forecasts and vegetation health to predict fire risk at subseasonal timescale in the Amazon. Environ Res Lett. 2022;17(7):074009. https://doi.org/10.1088/1748-9326/ac76d8.
96. Leblon B. Monitoring forest fire danger with remote sensing. Nat Hazards. 2005;35(3):343–59. https://doi.org/10.1007/s11069-004-1796-3.
97. Abdullah H, Darvishzadeh R, Skidmore AK, Heurich M. Sensitivity of Landsat-8 OLI and TIRS data to foliar properties of early stage bark beetle (Ips typographus, L.) infestation. Remote Sensing. 2019;11(4):398. https://doi.org/10.3390/rs11040398.
98. Sprintsin M, Chen JM, Czurylowicz P. Combining land surface temperature and shortwave infrared reflectance for early detection of mountain pine beetle infestations in western Canada. J Appl Remote Sens. 2011;5(1):053566. https://doi.org/10.1117/1.3662866.
99. Dinerstein E, Olson D, Joshi A, Vynne C, Burgess ND, Wikramanayake E, et al. An ecoregion-based approach to protecting half the terrestrial realm. Bioscience. 2017;67(6):534–45. https://doi.org/10.1093/biosci/bix014.
100. Zhong S, Di L, Sun Z, Xu Z, Guo L. Investigating the long-term spatial and temporal characteristics of vegetative drought in the contiguous United States. IEEE J Sel Top Appl Earth Observ Remote Sens. 2019;12(3):836–48. https://doi.org/10.1109/JSTARS.2019.2896159.

101. Shi S, Yao F, Zhang J, Yang S. Evaluation of temperature vegetation dryness index on drought monitoring over Eurasia. IEEE Access. 2020;8:30050–9. https://doi.org/10.1109/ACCESS.2020.2972271.
102. Wei W, Zhang J, Zhou L, Xie B, Zhou J, Li C. Comparative evaluation of drought indices for monitoring drought based on remote sensing data. Environ Sci Pollut Res. 2021;28(16):20408–25. https://doi.org/10.1007/s11356-020-12120-0.
103. Jiménez-Muñoz JC, Sobrino JA, Mattar C, Malhi Y. Spatial and temporal patterns of the recent warming of the Amazon forest. J Geophys Res: Atmospheres. 2013;118(11):5204–15. https://doi.org/10.1002/jgrd.50456.
104. Vilanova RS, Delgado RC, da Silva Abel EL, Teodoro PE, Silva Junior CA, Wanderley HS, et al. Past and future assessment of vegetation activity for the state of Amazonas-Brazil. Remote Sens Appl: Soc Environ. 2020;17:100278. https://doi.org/10.1016/j.rsase.2019.100278.
105. Mildrexler D, Yang Z, Cohen WB, Bell DM. A forest vulnerability index based on drought and high temperatures. Remote Sens Environ. 2016;173:314–25. https://doi.org/10.1016/j.rse.2015.11.024.
106. Lemon MGT, Allen ST, Edwards BL, King SL, Keim RF. Satellite-derived temperature data for monitoring water status in a floodplain forest of the Upper Sabine River, Texas. Southeast Nat. 2016;15(sp9):90–102. https://doi.org/10.1656/058.015.0sp911.
107. Decuyper M, Chávez RO, Čufar K, Estay SA, Clevers JGPW, Prislan P, et al. Spatio-temporal assessment of beech growth in relation to climate extremes in Slovenia – an integrated approach using remote sensing and tree-ring data. Agric For Meteorol. 2020;287:107925. https://doi.org/10.1016/j.agrformet.2020.107925.
108. Deshayes M, Guyon D, Jeanjean H, Stach N, Jolly A, Hagolle O. The contribution of remote sensing to the assessment of drought effects in forest ecosystems. Ann For Sci. 2006;63(6):579–95. https://doi.org/10.1051/forest:2006045.
109. Pierce LL, Running SW, Riggs GA. Remote detection of canopy water stress in coniferous forests using the NS001 thematic mapper simulator and the thermal infrared multispectral scanner. Photogramm Eng Remote Sens. 1990;56:579–86.
110. Alonzo M, Andersen H-E, Morton DC, Cook BD. Quantifying boreal forest structure and composition using UAV structure from motion. Forests. 2018;9(3):119. https://doi.org/10.3390/f9030119.
111. Brede B, Calders K, Lau A, Raumonen P, Bartholomeus HM, Herold M, et al. Non-destructive tree volume estimation through quantitative structure modelling: comparing UAV laser scanning with terrestrial LIDAR. Remote Sens Environ. 2019;233:111355. https://doi.org/10.1016/j.rse.2019.111355.
112. Qin H, Zhou W, Yao Y, Wang W. Individual tree segmentation and tree species classification in subtropical broadleaf forests using UAV-based LiDAR, hyperspectral, and ultrahigh-resolution RGB data. Remote Sens Environ. 2022;280:113143. https://doi.org/10.1016/j.rse.2022.113143.
113. Schiefer F, Kattenborn T, Frick A, Frey J, Schall P, Koch B, et al. Mapping forest tree species in high resolution UAV-based RGB-imagery by means of convolutional neural networks. ISPRS J Photogramm Remote Sens. 2020;170:205–15. https://doi.org/10.1016/j.isprsjprs.2020.10.015.
114. Ecke S, Dempewolf J, Frey J, Schwaller A, Endres E, Klemmt H-J, et al. UAV-based forest health monitoring: a systematic review. Remote Sensing. 2022;14(13):3205. https://doi.org/10.3390/rs14133205.
115. Dash JP, Watt MS, Pearse GD, Heaphy M, Dungey HS. Assessing very high resolution UAV imagery for monitoring forest health during a simulated disease outbreak. ISPRS J Photogramm Remote Sens. 2017;131:1–14. https://doi.org/10.1016/j.isprsjprs.2017.07.007.
116. Berra EF, Gaulton R, Barr S. Assessing spring phenology of a temperate woodland: a multiscale comparison of ground, unmanned aerial vehicle and Landsat satellite observations. Remote Sens Environ. 2019;223:229–42. https://doi.org/10.1016/j.rse.2019.01.010.
117. Park JY, Muller-Landau HC, Lichstein JW, Rifai SW, Dandois JP, Bohlman SA. Quantifying leaf phenology of individual trees and species in a tropical forest using unmanned aerial vehicle (UAV) images. Remote Sensing. 2019;11(13):1534. https://doi.org/10.3390/rs11131534.
118. de Sá NC, Castro P, Carvalho S, Marchante E, López-Núñez FA, Marchante H. Mapping the flowering of an invasive plant using unmanned aerial vehicles: is there potential for biocontrol monitoring? Front Plant Sci. 2018;9:293. https://doi.org/10.3389/fpls.2018.00293.
119. Smigaj M, Gaulton R. Capturing hedgerow structure and flowering abundance with UAV remote sensing. Remote Sens Ecol Conserv. 2021;7(3):521–33. https://doi.org/10.1002/rse2.208.
120. Zhang L, Niu Y, Zhang H, Han W, Li G, Tang J, Peng X. Maize Canopy Temperature Extracted From UAV Thermal and RGB Imagery and Its Application in Water Stress Monitoring. Front Plant Sci. 2019;10:1270. https://doi.org/10.3389/fpls.2019.01270.
121. Bian J, Zhang Z, Chen J, Chen H, Cui C, Li X, et al. Simplified evaluation of cotton water stress using high resolution unmanned aerial vehicle thermal imagery. Remote Sensing. 2019;11(3):267. https://doi.org/10.3390/rs11030267.
122. Drake PL, Callow NJ, Leopold M, Pires RN, Veneklaas EJ. Thermal imagery of woodland tree canopies provides new insights into drought-induced tree mortality. Sci Total Environ. 2022;834:155395. https://doi.org/10.1016/j.scitotenv.2022.155395.
123. Wang J, Meng S, Lin Q, Liu Y, Huang H. Detection of Yunnan pine shoot beetle stress using UAV-based thermal imagery and LiDAR. Appl Sci. 2022;12(9):4372. https://doi.org/10.3390/app12094372.
124. Aubrecht DM, Helliker BR, Goulden ML, Roberts DA, Still CJ, Richardson AD. Continuous, long-term, high-frequency thermal imaging of vegetation: uncertainties and recommended best practices. Agric For Meteorol. 2016;228–229:315–26. https://doi.org/10.1016/j.agrformet.2016.07.017.
125. Kim Y, Still CJ, Hanson CV, Kwon H, Greer BT, Law BE. Canopy skin temperature variations in relation to climate, soil temperature, and carbon flux at a ponderosa pine forest in central Oregon. Agric For Meteorol. 2016;226–227:161–73. https://doi.org/10.1016/j.agrformet.2016.06.001.
126. Still CJ, Page G, Rastogi B, Griffith DM, Aubrecht DM, Kim Y, et al. No evidence of canopy-scale leaf thermoregulation to cool leaves below air temperature across a range of forest ecosystems. Proc Natl Acad Sci. 2022;119(38):e2205682119. https://doi.org/10.1073/pnas.2205682119.
127. Lapidot O, Ignat T, Rud R, Rog I, Alchanatis V, Klein T. Use of thermal imaging to detect evaporative cooling in coniferous and broadleaved tree species of the Mediterranean maquis. Agric For Meteorol. 2019;271:285–94. https://doi.org/10.1016/j.agrformet.2019.02.014.
128. Pau S, Detto M, Kim Y, Still CJ. Tropical forest temperature thresholds for gross primary productivity. Ecosphere. 2018;9(7):e02311. https://doi.org/10.1002/ecs2.2311.
129. Nanda MK, Giri U, Bera N. Canopy temperature-based water stress indices: potential and limitations. In: Bal SK, Mukherjee J, Choudhury BU, Dhawan AK, editors. Advances in crop environment interaction. Singapore: Springer Singapore; 2018. p. 365–85. https://doi.org/10.1007/978-981-13-1861-0_14.

130. Messina G, Modica G. Applications of UAV thermal imagery in precision agriculture: state of the art and future research outlook. Remote Sensing. 2020;12(9):1491. https://doi.org/10.3390/rs12091491.
131. Idso SB, Jackson RD, Pinter PJ, Reginato RJ, Hatfield JL. Normalizing the stress-degree-day parameter for environmental variability. Agric Meteorol. 1981;24:45–55. https://doi.org/10.1016/0002-1571(81)90032-7.
132. Idso SB. Non-water-stressed baselines: a key to measuring and interpreting plant water stress. Agric Meteorol. 1982;27(1):59–70. https://doi.org/10.1016/0002-1571(82)90020-6.
133. Pascolini-Campbell M, Lee C, Stavros N, Fisher JB. ECOSTRESS reveals pre-fire vegetation controls on burn severity for Southern California wildfires of 2020. Glob Ecol Biogeogr. 2022;31(10):1976–89. https://doi.org/10.1111/geb.13526.
134. Yang Y, Anderson MC, Gao F, Wood JD, Gu L, Hain C. Studying drought-induced forest mortality using high spatiotemporal resolution evapotranspiration data from thermal satellite imaging. Remote Sens Environ. 2021;265:112640. https://doi.org/10.1016/j.rse.2021.112640. **This article shows the utility of evapotranspiration metrics derived from thermal imagery for detecting drought impacts.**
135. Guillevic P, Gastellu-Etchegorry JP, Demarty J, Prévot L. Thermal infrared radiative transfer within three-dimensional vegetation covers. J Geophys Res. 2003;108(D8):4248. https://doi.org/10.1029/2002JD002247.
136. Calders K, Origo N, Burt A, Disney M, Nightingale J, Raumonen P, et al. Realistic forest stand reconstruction from terrestrial LiDAR for radiative transfer modelling. Remote Sensing. 2018;10(6):933. https://doi.org/10.3390/rs10060933.
137. Kobayashi H, Iwabuchi H. A coupled 1-D atmosphere and 3-D canopy radiative transfer model for canopy reflectance, light environment, and photosynthesis simulation in a heterogeneous landscape. Remote Sens Environ. 2008;112(1):173–85. https://doi.org/10.1016/j.rse.2007.04.010.
138. Cao B, Liu Q, Du Y, Roujean J-L, Gastellu-Etchegorry J-P, Trigo IF, et al. A review of earth surface thermal radiation directionality observing and modeling: historical development, current status and perspectives. Remote Sens Environ. 2019;232:111304. https://doi.org/10.1016/j.rse.2019.111304. **Recommended resource for background information on radiative transfer modelling in the thermal domain.**
139. Bian Z, Wu S, Roujean J-L, Cao B, Li H, Yin G, et al. A TIR forest reflectance and transmittance (FRT) model for directional temperatures with structural and thermal stratification. Remote Sens Environ. 2022;268:112749. https://doi.org/10.1016/j.rse.2021.112749.
140. Hernández-Clemente R, Hornero A, Mottus M, Penuelas J, González-Dugo V, Jiménez JC, et al. Early diagnosis of vegetation health from high-resolution hyperspectral and thermal imagery: lessons learned from empirical relationships and radiative transfer modelling. Curr For Rep. 2019;5(3):169–83. https://doi.org/10.1007/s40725-019-00096-1. **A review highlighting how different remote sensing modalities can be combined for improved vegetation health monitoring.**
141. Kobayashi H, Baldocchi DD, Ryu Y, Chen Q, Ma S, Osuna JL, et al. Modeling energy and carbon fluxes in a heterogeneous oak woodland: a three-dimensional approach. Agric For Meteorol. 2012;152:83–100. https://doi.org/10.1016/j.agrformet.2011.09.008.
142. Wang Y, Kallel A, Yang X, Regaieg O, Lauret N, Guilleux J, et al. DART-Lux: an unbiased and rapid Monte Carlo radiative transfer method for simulating remote sensing images. Remote Sens Environ. 2022;274:112973. https://doi.org/10.1016/j.rse.2022.112973.
143. Goodenough AA, Brown SD. DIRSIG5: next-generation remote sensing data and image simulation framework. IEEE J Select Top Appl Earth Obs Remote Sens. 2017;10(11):4818–33. https://doi.org/10.1109/JSTARS.2017.2758964.
144. Baldocchi D, Meyers T. On using eco-physiological, micrometeorological and biogeochemical theory to evaluate carbon dioxide, water vapor and trace gas fluxes over vegetation: a perspective. Agric For Meteorol. 1998;90(1):1–25. https://doi.org/10.1016/S0168-1923(97)00072-5.
145. Gastellu-Etchegorry JP, Demarez V, Pinel V, Zagolski F. Modeling radiative transfer in heterogeneous 3-D vegetation canopies. Remote Sens Environ. 1996;58(2):131–56. https://doi.org/10.1016/0034-4257(95)00253-7.
146. Mason J, Schott J, Rankin-Parobek D. radiometric integrity of RIT's synthetic image generation model, DIRSIG, Proc. SPIE 2223, Characterization and Propagation of Sources and Backgrounds, 1994; https://doi.org/10.1117/12.177938.
147. Berni JAJ, Zarco-Tejada PJ, Suarez L, Fereres E. Thermal and narrowband multispectral remote sensing for vegetation monitoring from an unmanned aerial vehicle. IEEE Trans Geosci Remote Sens. 2009;47(3):722–38. https://doi.org/10.1109/TGRS.2008.2010457.
148. Nishar A, Richards S, Breen D, Robertson J, Breen B. Thermal infrared imaging of geothermal environments and by an unmanned aerial vehicle (UAV): a case study of the Wairakei – Tauhara geothermal field, Taupo, New Zealand. Renewable Energy. 2016;86:1256–64. https://doi.org/10.1016/j.renene.2015.09.042.
149. Hoegner L, Tuttas S, Xu Y, Eder K, Stilla U. Evaluation of methods for coregistration and fusion of RPAS-baseD 3D point clouds and thermal infrared images. Int Arch Photogramm Remote Sens Spatial Inf Sci. 2016. https://doi.org/10.5194/isprs-archives-XLI-B3-241-2016.
150. Maset E, Fusiello A, Crosilla F, Toldo R, Zorzetto D. Photogrammetric 3D building reconstruction from thermal images. ISPRS Ann Photogramm Remote Sens Spat Inform Sci. 2017;4:25. https://doi.org/10.5194/isprs-annals-IV-2-W3-25-2017.
151. Ham Y, Golparvar-Fard M. An automated vision-based method for rapid 3D energy performance modeling of existing buildings using thermal and digital imagery. Adv Eng Inform. 2013;27(3):395–409. https://doi.org/10.1016/j.aei.2013.03.005.
152. Webster C, Westoby M, Rutter N, Jonas T. Three-dimensional thermal characterization of forest canopies using UAV photogrammetry. Remote Sens Environ. 2018;209:835–47. https://doi.org/10.1016/j.rse.2017.09.033.
153. Javadnejad F, Gillins DT, Parrish CE, Slocum RK. A photogrammetric approach to fusing natural colour and thermal infrared UAS imagery in 3D point cloud generation. Int J Remote Sens. 2020;41(1):211–37. https://doi.org/10.1080/01431161.2019.1641241.
154. Smigaj M, Gaulton R, Barr S, Suarez J. Investigating the performance of a low-cost thermal imager for forestry applications: SPIE; 2016. https://doi.org/10.1117/12.2241417.
155. Mesas-Carrascosa F-J, Pérez-Porras F, Meroño de Larriva JE, Mena Frau C, Agüera-Vega F, Carvajal-Ramírez F, et al. Drift correction of lightweight microbolometer thermal sensors on-board unmanned aerial vehicles. Remote Sensing. 2018;10(4):615. https://doi.org/10.3390/rs10040615.
156. Virtue J, Turner D, Williams G, Zeliadt S, McCabe M, Lucieer A. Thermal sensor calibration for unmanned aerial systems using an external heated shutter. Drones. 2021;5(4):119. https://doi.org/10.3390/drones5040119.
157. Gómez-Candón D, Virlet N, Labbé S, Jolivot A, Regnard J-L. Field phenotyping of water stress at tree scale by UAV-sensed imagery: new insights for thermal acquisition and calibration.

Precision Agric. 2016;17(6):786–800. https://doi.org/10.1007/s11119-016-9449-6.
158. Boubanga-Tombet S, Huot A, Vitins I, Heuberger S, Veuve C, Eisele A, et al. Thermal infrared hyperspectral imaging for mineralogy mapping of a mine face. Remote Sensing. 2018;10(10):1518. https://doi.org/10.3390/rs10101518.
159. Vaughan RG, Hook SJ, Calvin WM, Taranik JV. Surface mineral mapping at Steamboat Springs, Nevada, USA, with multi-wavelength thermal infrared images. Remote Sens Environ. 2005;99(1):140–58. https://doi.org/10.1016/j.rse.2005.04.030.
160. Reath KA, Ramsey MS. Exploration of geothermal systems using hyperspectral thermal infrared remote sensing. J Volcanol Geoth Res. 2013;265:27–38. https://doi.org/10.1016/j.jvolgeores.2013.08.007.
161. Black M, Riley TR, Ferrier G, Fleming AH, Fretwell PT. Automated lithological mapping using airborne hyperspectral thermal infrared data: a case study from Anchorage Island, Antarctica. Remote Sens Environ. 2016;176:225–41. https://doi.org/10.1016/j.rse.2016.01.022.
162. Ullah S, Schlerf M, Skidmore AK, Hecker C. Identifying plant species using mid-wave infrared (2.5–6μm) and thermal infrared (8–14μm) emissivity spectra. Remote Sens Environ. 2012;118:95–102. https://doi.org/10.1016/j.rse.2011.11.008.
163. Ribeiro da Luz B, Crowley JK. Identification of plant species by using high spatial and spectral resolution thermal infrared (8.0–13.5μm) imagery. Remote Sens Environ. 2010;114(2):404–13. https://doi.org/10.1016/j.rse.2009.09.019.
164. Buitrago MF, Groen TA, Hecker CA, Skidmore AK. Changes in thermal infrared spectra of plants caused by temperature and water stress. ISPRS J Photogramm Remote Sens. 2016;111:22–31. https://doi.org/10.1016/j.isprsjprs.2015.11.003.
165. Gerhards M, Rock G, Schlerf M, Udelhoven T. Water stress detection in potato plants using leaf temperature, emissivity, and reflectance. Int J Appl Earth Obs Geoinf. 2016;53:27–39. https://doi.org/10.1016/j.jag.2016.08.004.
166. Fabre S, Lesaignoux A, Olioso A, Briottet X. Influence of water content on spectral reflectance of leaves in the 3–15- μm domain. IEEE Geosci Remote Sens Lett. 2011;8(1):143–7. https://doi.org/10.1109/LGRS.2010.2053518.
167. Kirkland L, Herr K, Keim E, Adams P, Salisbury J, Hackwell J, et al. First use of an airborne thermal infrared hyperspectral scanner for compositional mapping. Remote Sens Environ. 2002;80(3):447–59. https://doi.org/10.1016/S0034-4257(01)00323-6.
168. Smigaj M, Gaulton R, Suárez JC, Barr SL. Combined use of spectral and structural characteristics for improved red band needle blight detection in pine plantation stands. For Ecol Manage. 2019;434:213–23. https://doi.org/10.1016/j.foreco.2018.12.005.
169. Campbell MJ, Dennison PE, Tune JW, Kannenberg SA, Kerr KL, Codding BF, et al. A multi-sensor, multi-scale approach to mapping tree mortality in woodland ecosystems. Remote Sens Environ. 2020;245:111853. https://doi.org/10.1016/j.rse.2020.111853.
170. Shendryk I, Broich M, Tulbure MG, McGrath A, Keith D, Alexandrov SV. Mapping individual tree health using full-waveform airborne laser scans and imaging spectroscopy: a case study for a floodplain eucalypt forest. Remote Sens Environ. 2016;187:202–17. https://doi.org/10.1016/j.rse.2016.10.014.
171. Berger K, Machwitz M, Kycko M, Kefauver SC, Van Wittenberghe S, Gerhards M, et al. Multi-sensor spectral synergies for crop stress detection and monitoring in the optical domain: a review. Remote Sens Environ. 2022;280:113198. https://doi.org/10.1016/j.rse.2022.113198.